AD_____

Award Number: DAMD17-94-J-4284

TITLE: Role of CD44 in Tumor Progression

PRINCIPAL INVESTIGATOR: Charles Underhill, Ph.D.

CONTRACTING ORGANIZATION: Georgetown University
Washington, DC 20057

REPORT DATE: September 1999

TYPE OF REPORT: Final

PREPARED FOR: U.S. Army Medical Research and Materiel Command
Fort Detrick, Maryland 21702-5012

DISTRIBUTION STATEMENT: Approved for public release
distribution unlimited

The views, opinions and/or findings contained in this report are those of the author(s) and should not be construed as an official Department of the Army position, policy or decision unless so designated by other documentation.

REPORT DOCUMENTATION PAGE

Form Approved
OMB No. 074-0188

1. AGENCY USE ONLY (Leave blank)	2. REPORT DATE	3. REPORT TYPE AND DATES COVERED
	September 1999	Final (01 Sep 94 - 31 Aug 99)

4. TITLE AND SUBTITLE
Role of CD44 in Tumor Progression

5. FUNDING NUMBERS
DAMD17-94-J-4284

6. AUTHOR(S)
Charles Underhill, Ph.D.

7. PERFORMING ORGANIZATION NAME(S) AND ADDRESS(ES)
Georgetown University
Washington, DC 20057

e-mail:
underhic@gunet.georgetown.edu

8. PERFORMING ORGANIZATION REPORT NUMBER

9. SPONSORING / MONITORING AGENCY NAME(S) AND ADDRESS(ES)
U.S. Army Medical Research and Materiel Command
Fort Detrick, Maryland 21702-5012

10. SPONSORING / MONITORING AGENCY REPORT NUMBER

11. SUPPLEMENTARY NOTES

12a. DISTRIBUTION / AVAILABILITY STATEMENT
Approved for public release
distribution unlimited

12b. DISTRIBUTION CODE

13. ABSTRACT *(Maximum 200 Words)*

This project is concerned with the role of hyaluronan (HA) in tumor progression. Initially, we postulated that CD44 and HA played a role in angiogenesis. However, our studies suggested that this hypothesis was probably not correct. Subsequently, we attempted to target tumor-associated HA with an HA-binding complex (HAbc) that we isolated from cartilage by affinity chromatography. We found that the HAbc was able to block the growth of tumors cells in mice as well as in the chorioallantoic membrane (CAM) of chicken embryos. Furthermore, when HAbc was added to the medium of cultured endothelial cells, growth of these cells was inhibited in a dose-dependent fashion. Staining of these endothelial cells with Hoechst dye and analysis by flow cytometry suggested that this effect was due to the induction of apoptosis. In addition, when HAbc was injected i.v. into 10 day chicken embryos, it inhibited VEGF-induced angiogenesis in the CAM, indicative of anti-angiogenic activity. In each case, the effect was blocked by either heat-inactivation of the preparation or by premixing it with HA. Collectively, these results suggest that the binding of HAbc to HA of endothelial cells and induces apoptosis in these cells that, in turn, inhibits tumor vascularization and growth.

14. SUBJECT TERMS
Breast Cancer, angiogenesis, hyaluronan, cartilage, endothelial cells

15. NUMBER OF PAGES
60

16. PRICE CODE

17. SECURITY CLASSIFICATION OF REPORT	18. SECURITY CLASSIFICATION OF THIS PAGE	19. SECURITY CLASSIFICATION OF ABSTRACT	20. LIMITATION OF ABSTRACT
Unclassified	Unclassified	Unclassified	Unlimited

FOREWORD

Opinions, interpretations, conclusions and recommendations are those of the author and are not necessarily endorsed by the U.S. Army.

_√CBH Where copyrighted material is quoted, permission has been obtained to use such material.

____ Where material from documents designated for limited distribution is quoted, permission has been obtained to use the material.

____ Citations of commercial organizations and trade names in this report do not constitute an official Department of Army endorsement or approval of the products or services of these organizations.

_√CBH In conducting research using animals, the investigator(s) adhered to the "Guide for the Care and Use of Laboratory Animals," prepared by the Committee on Care and use of Laboratory Animals of the Institute of Laboratory Resources, national Research Council (NIH Publication No. 86-23, Revised 1985).

_√CBH For the protection of human subjects, the investigator(s) adhered to policies of applicable Federal Law 45 CFR 46.

_√CBH In conducting research utilizing recombinant DNA technology, the investigator(s) adhered to current guidelines promulgated by the National Institutes of Health.

_√CBH In the conduct of research utilizing recombinant DNA, the investigator(s) adhered to the NIH Guidelines for Research Involving Recombinant DNA Molecules.

_√CBH In the conduct of research involving hazardous organisms, the investigator(s) adhered to the CDC-NIH Guide for Biosafety in Microbiological and Biomedical Laboratories.

Charles Underhill 9/29/99

PI - Signature Date

TABLE OF CONTENTS:

INTRODUCTION:

The present research project is concerned with the interaction between tumor cells and hyaluronan (HA), one of the major components of the extracellular matrix. HA is a large, negatively-charged carbohydrate that functions to maintain spaces between cells that are important for the diffusion of nutrients (1, 2). In previous studies, we had found that many tumor cells express CD44, a cell surface protein that can bind and HA and plays a critical role in its degradation (3-5). Initially, our goal was to examine the role of CD44 and HA in the vascularization of tumors (Tasks 1-4). Unfortunately, the results of these studies indicated that CD44 probably did not play a major role in regulating angiogenesis, and consequently we changed direction. Since we had observed that many tumors produced large amounts of HA, we proposed to target this HA with an HA-binding complex (HAbc) derived from cartilage and coupled to a chemotherapeutic agent (Tasks 5-7). However, in the course of these studies, we found that the HAbc by itself (i.e. without the chemotherapeutic agent) had anti-tumor activity. These results were completely unexpected and very exciting. Consequently, during the past year we directed most of our efforts reproducing and extending these initial observations (Task 8).

Each of the approved tasks are listed as follows:

1. *Examine the effect of CD44 expression of the vascularization of tumors:* To determine if the expression of CD44 leads to an increase in the vascular supply, we transfected cancer cells with a CD44 expression vector, and inject these cells into nude mice. We then proposed to examine the xenografts derived from the CD44-positive cells for blood vessels.
2. *Determine the effects of various agents on the vascularization of tumors:* Tumor cells growing on the chorioallantoic membrane of chicken embryos were exposed to hyaluronidase, to determine if this influenced vascularization
3. *Examine the expression of CD44 in primary and secondary tumors of transgenic mice:* To determine if the expression of CD44 imparts a growth advantage to these cells, we examined both primary and secondary tumors formed by transgenic strains of mice that spontaneously develop breast tumors.
4. *Survey specimens of human breast tumor for the presence of CD44, HA and vascular endothelial cells:* Specimens of human breast cancer, were evaluated for the expression of CD44, HA and endothelial cells to determine if they were correlated with the metastatic potential.
5. *To examine various types of lung metastases for the expression of HA:* In previous experiments, we observed that HA was often associated with lung metastases. To determine if this phenomenon is universal, we examined a number of other systems involving metastases to the lungs.
6. *To test the possibility of using HAbc to target lung metastases:* To determine if the tumor-associated HA can be targeted with HAbc, we injected a biotinylated form of this complex (b-PG) into mice that had tumor metastases and determine its distribution
7. *To examine the effects of HAbc coupled to MTX on cultured tumor cells:* To test the feasibility of using derivatives of HAbc to deliver chemotherapeutic drugs to tumor cells, we coupled the chemotherapeutic agent methotrexate (MTX) to HAbc and tested its ability to kill tumor cells in culture.
8. *To determine the effect of HAbc on tumor growth*: For this study, tumor cells were injected into mice or applied to the chorioallantoic membrane of chicken embryos and the effect of HAbc on the growth of these cells was determined. In each case, the tumor cell growth was inhibited by the HAbc, and this inhibition was blocked if the HAbc was heat inactivated or pretreated with HA. Subsequent studies suggested that the HAbc was acting by blocking angiogenesis of the tumors.

BODY

During the previous funding period, we concentrated our efforts on examining the anti-tumor activity of an HA-binding complex (HAbc) derived from cartilage by affinity chromatography on HA-Sepharose. We initially discovered the anti-tumor properties effects of this complex in experiments designed to target HA associated with tumor cells. Our original idea was to couple HAbc to a chemotherapeutic agent such as methotrexate (MTX) and then inject this preparation into animals with tumors. It was our hope that the MTX-HAbc would bind to tumor-associated HA, be taken up by the tumor cells and cause their death. As a control for these studies, we tested the HAbc preparation directly in animal models of metastasis. Unexpectedly, we found that the HAbc by itself (i.e. without the chemotherapeutic agent) significantly down-regulated tumor growth. During the past year, we have confirmed and expanded these initial results. In particular, we have found that the HAbc also blocks the growth of tumor cells in the chicken chorioallantoic membrane (CAM) system. In addition, we have found that the HAbc appears to be acting by inhibiting tumor angiogenesis. These new results will be described in greater detail in the new Task 8.

In the following sections, we will discuss the results of both the old and the new Tasks. Since most of the old tasks have been discontinued due to disappointing results or have been incorporated into the new Tasks, we will present only brief summaries of these. In the case of the new Task 8, concerning the anti-tumor effects of HAbc, these recent results will be described in greater detail. As indicated above, we are very excited about the potential significance and implications of the phenomenon described in Task 8.

Task 1: Examine the effect of CD44 expression on the vascularization of tumors: The purpose of this study was to test the hypothesis that CD44 enhances the vascularization of tumors. To accomplish this, we proposed to transfect human breast cancer cell lines with a CD44 expression vector, grow these cells in nude mice, and then analyze the resulting xenografts for endothelial cells.

1.1. Preparation and characterization of CD44 transfected cells: We transfected a number of human breast cancer cell lines (ZR-751, MCF-7, and ML-20) with an expression vector for human CD44 and found that they gained the ability to bind and degrade HA in a CD44-dependent fashion as we had predicted. However, when these cells were injected into the fat pads of nude mice, none of them grew despite repeated attempts under a variety of conditions (i.e. with and without Metragel and estrogen). Thus, we have been unable to test the hypothesis that the expression of CD44 allows the tumor cells to degrade the HA in the extracellular matrix and stimulate angiogenesis. We conclude from this that transfection with CD44 does not confer increased growth potential in nude mice, at least in the case of the human breast cancer cell lines. This is in keeping with the results from other laboratories that increased metastatic potential following transfection with CD44 expression vectors is very dependent upon the cell type. At this point, we have attempted this experiment with all of the appropriate human breast cancer cell lines at our disposal.

1.2. Conclusions: The results of these experiments suggest that CD44 does not play a significant role in promoting vascularization of breast cancer tumors.

Task 2. Determine the effects of various agents on the vascularization of tumors expressing CD44: The purpose of this set of experiments was to determine if vascularization of xenografts could be blocked by antibodies to CD44 or enhanced by fragments of HA or HAase. As described above, we now believe that CD44 on the surfaces of tumor cells does not play an important role in vascularization. For this

reason, we have not further examined the effects of CD44. However, we have recently tested the effects of HAase on the growth of tumor cells which is described in the following section.

2.1. The effects of HAase on the growth of B16BL6 cells on the CAM. In this model system, the chorioallantoic membranes (CAM) of ten day old chicken eggs were exposed and then 1 x 10^6 B16BL6 cells were placed on top of it (see section 8.3 for more details of this assay). One day later, the embryos were injected with preparations of either testicular or *streptomyces* HAase. After one week, the tumor masses were excised and weighed. As shown in Fig. 1, the HAase treatment significantly increase the size of the B16BL6 xenografts as compared to controls injected with saline or heat-inactivated HAase. Histochemical staining of the xenografts indicated that the central region of the HAase treated samples contained large pools of erythrocytes that were absent from the control sections. However, when the embryos were injected i.v. with India ink 30 minutes prior to sacrifice, the ink did not enter these large pools of blood, suggesting that they were cut off from the circulation.

2.2. Conclusions: Based on these results, we believe that HAase treatment caused spaces to open up in the tumor tissue and allows blood to enter these regions. However, these spaces do not exhibit a rapid flow of blood suggesting that they are cut off from the regular circulation. The most likely explanation is that these spaces are more like bleeding within the tumor. Regardless of the cause, the net effect was that HAase treatment caused an increase in the growth of the tumor cells. Thus, our original hypothesis that HA plays an important role in vascularization seems to be correct. We are currently testing other tumors to determine if HAase has a similar effect.

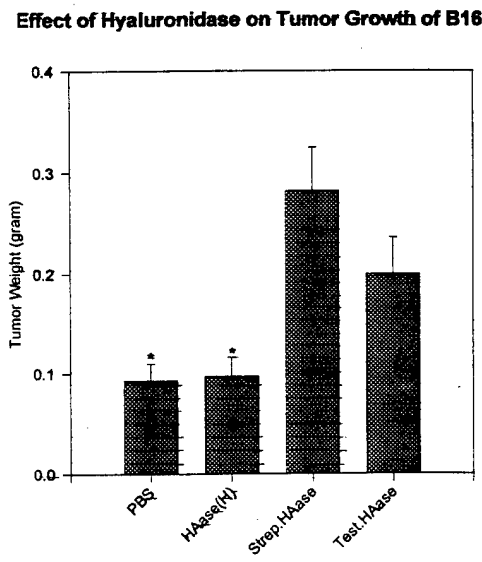

Fig. 1. The effect of HAase on the growth of B16BL6 cells on the chicken CAM. The chicken embryos were given a single injected of saline (PBS); heat-inactivated testicular HAase (HAase(H)), Streptomyces HAase (Strep. HAase) and testicular HAase (Test. HAase). Six days later, the B16BL6 tumor masses were weighed.

Task 3. Examine the expression of CD44 in primary and secondary tumors of transgenic mice: The purpose of this set of experiments was to compare primary versus secondary tumors with respect to the expression of CD44 and HA. For this, we examined a strain of mice that has been transfected with a polyomavirus middle T oncogene under the control of a mouse mammary tumor virus promoter/enhancer (6). This transgenic strain of mice forms multifocal mammary adenocarcinomas that metastasize to the lungs at a high frequency. The results of this study form the foundation of the new Tasks 5, 6 and 7.

3.1. Distribution of HA and CD44 in primary and secondary tumors: A mouse with a large tumor load was sacrificed and both the primary tumor and the lungs were removed and fixed overnight in formaldehyde. The tissues were then embedded in polyester wax, which helps to preserve the antigenicity (7) and then stained for both CD44 using the KM-201 mAb and HA using the b-HAbc probe which is described below (14, 22).

The primary tumor present in the breast tissue was heterogeneous with respect to the expression of both CD44 and HA. The amount of CD44 appeared to be highest at the edge of the primary tumor and decrease towards the center of the mass. A similar type of pattern was observed with the HA, with the highest concentration again towards the edge of the tumor.

We then examined the distribution of CD44 in secondary tumors that were present in the lung tissue, and found that its distribution was similar to that of the original tumor, with positive staining on the cells located on the periphery and much less staining in the center of the tumor mass. In addition, a large number of macrophages that also stain for CD44 were apparent in the vicinity of the tumor, while adjacent sections of normal lung tissue contained far fewer macrophages. This was consistent with other studies showing that many tumors are associated with macrophages (8, 9). Interestingly, it appeared that many of these macrophages are aggregated, perhaps as a response to elevated levels of HA.

When the lung tissue was stained for HA, large amounts of HA were present in the alveolar tissue surrounding the tumor mass (Fig. 2 A). In contrast, adjacent normal lung tissue contained low levels of HA, most of which was present in the connective tissue surrounding the major blood vessels and air passage ways (Fig. 2 B). It appeared that while some of the HA was associated directly with the tumor itself, much of the HA was located some distance away from the tumor mass in the surrounding normal tissue, suggesting that it was derived from the normal lung tissue perhaps as a result of a localized immune response. Along these lines, other studies have shown that an inflammatory response in the lungs results in increased levels of HA (10-12). It is also possible that this HA accounts for the observation described above that many of the macrophages in the vicinity of the tumor were clumped together, since we had previously shown that HA can induce these cells to aggregate by interacting with CD44 present on these cells (13).

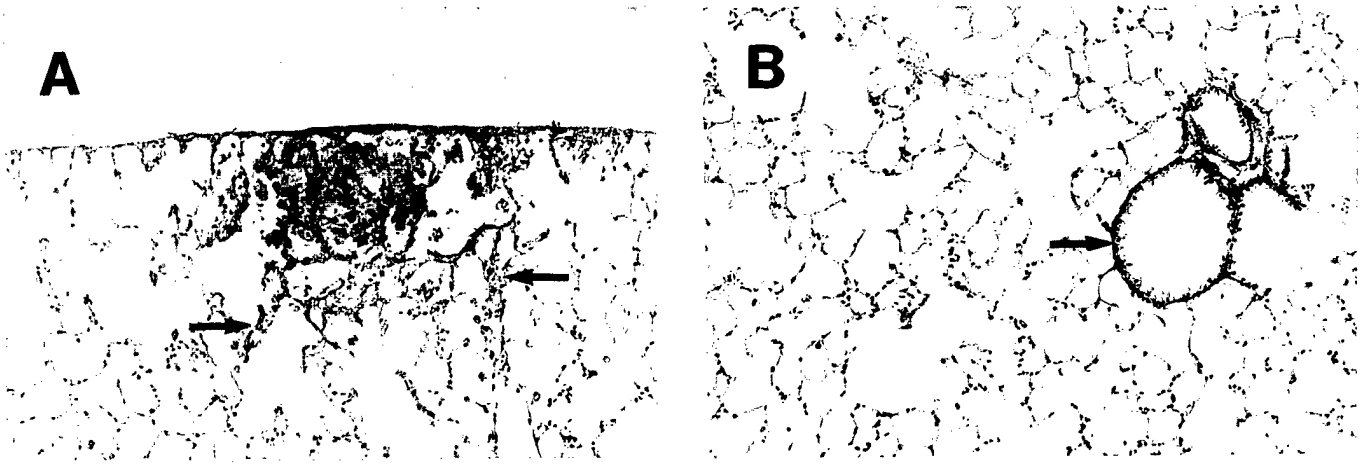

Fig. 2. The distribution of HA in a lung metastasis from a transgenic mouse. (A) A section of the lungs shows that large amounts of HA are associated with the tumor mass. Much of this HA is located some distance from the tumor in the normal lung tissue (see arrows). (B) An adjacent section of normal lung tissue shows that HA is generally restricted to the adventitia of large blood vessels and air passage ways.

This high levels of HA associated with the metastatic tumors in the lungs may have important implications. In particular, it suggested the possibility that this HA could be used to locate and target tumor metastases. This could be accomplished with the HAbc from cartilage that we had used previously as a histochemical stain for HA. This HAbc probe consists of a trypsin fragment of the aggrecan molecule along with an associated link protein that bind to hyaluronan with both high affinity and specificity (14, 22). It may be possible to attach chemotherapeutic agents to this HAbc and inject this into individuals with tumors.

3.2. Conclusions: High concentration of HA are often associated with tumor metastasis and could potentially serve as a target of chemotherapeutic intervention (see Tasks 5, 6, 7 and 8).

Task 4. Survey specimens of human breast tumor for the presence of CD44, HA and vascular endothelial cells: The purpose of this study was to determine if the expression of CD44 and HA was correlated with the distribution of blood vessels and if this could be used as a diagnostic indicator of tumor behavior. For this, we have made use of the Breast Cancer tumor bank which is one of the core facilitates of the Lombardi Cancer Center. Samples were selected from the tumor bank based upon the availability of specimens representing a spectrum of invasive tissue types including normal, ductal carcinoma *in situ*, and metastasis in the lymph nodes.

4.1. Distribution of HA and CD44 in breast cancers: When we examined normal breast tissue, we found that small amounts of CD44 were associated with the ductal cells and that HA was present in the stroma immediately surrounding the glandular epithelium, but was reduced or absent in regions located a short distance from the epithelium. In regions of invasive carcinoma and ductal carcinoma *in situ*, the tumor cells expressed high levels of CD44 and high levels of HA were associated with the surrounding stroma but was generally absent from the tumor mass. Finally, in the case of secondary tumors present in the lymph nodes, the expression of both CD44 and HA was variable. Taken together, these results indicate that while CD44 was not consistently associated with metastatic tumors, it was associated with the presence or absence of HA in the tumor mass.

Subsequently, we have extended this study to examine the distribution of both HA blood vessels (endothelial cells). Paraffin sections of human breast cancer from the core facilitates of the Lombardi Cancer Center were simultaneously stained for both HA and endothelial cells. The association between HA and endothelial cells was also found to be quite variable. In one tumor sample, blood vessels were present in the stroma surrounding the tumors that contain very little HA. However, in another tumor sample, there were large numbers of capillaries in matrix that is rich in HA. Thus, there is not a consistent correlation between the expression of HA and the presence or absence of blood vessels. However, this does not necessarily disprove the hypothesis that HA is involved in angiogenesis, since the HA may have been there originally when the blood vessels were initially formed and then subsequently lost. Thus, it is unclear if the distribution of HA has any predictive value in determining tumor angiogenesis.

4.2. Conclusions: While HA is often associated with endothelial cells in tumor tissue, the pattern was variable and consequently, it was difficult to draw any firm conclusions.

Task 5: To examine various types of lung metastases for the expression of HA: The purpose of this set of experiments was to determine if metastases to the lungs are associated with increased levels of HA in the surrounding tissue. While this was clearly the case for the transgenic mouse described in Task 3, the question remained as to whether or not this is a generalized phenomenon for all forms of lung metastases. To answer this question, we examined the nude mice that had been given injections of human breast cancer cell lines as well as lung biopsies containing metastases from human patients suffering from breast cancer

5.1. Distribution of HA in xenografts of human breast cancer cells in nude mice: In these experiments, MDA-231 and Hs578T cells (human breast cancer cell lines) were injected into the tail vein of nude mice and after one week, the mice were sacrificed and the lung tissue was collected. The lung tissue was embedded in paraffin, processed for histology and then stained for HA using the b-HAbc probe. The

results showed that large amounts of HA staining were associated with the tumor nodules in the lungs. In these cases, the HA appeared to be present in the normal tissue surround the tumor. Similar results were obtained when we examined biopsies of lung tissues from human patients suffering from breast cancer (from the core facilitates of the Lombardi Cancer Center). In most, but not all cases, elevated levels of HA were present in the normal stroma surrounding the tumors. We believe that the more advanced the tumor is, the less likely that it will be associated with HA.

Similar results were obtained when we examined several different models of tumor metastasis. In most, but not all cases, we observed that large amounts of HA surrounded tumor nodules present in the lungs. In general, greater amounts of HA tended to be associated with newly formed tumors and much less with those that had been present longer. These results suggest that when tumor cells initially metastasize to the lungs, they initiate a response that induces the synthesis of HA.

At present the nature of the signal leading to the increase in HA production is not clear. One possibility is that the tumor cells initiates an immune response in the lung tissue that causes the normal lung cells to produce HA. This is consistent with previous studies that have found that inflammation in the lungs results in an increase in the production of HA (10-12). Along these lines, in preliminary studies we have found that dexamethasone treatment tends to down-regulate the HA associated with lung metastases, suggesting that it is part of an immune response. Interesting, dexamethasone also stimulated the growth of tumors in the treated animals.

5.3. Conclusions: HA is often associated with both primary and secondary tumors and may be suitable as a target for chemotherapeutic intervention.

Task 6: To test the possibility of using HAbc to target lung metastases: The fact that HA is often associated with lung metastases suggested the possibility that it might be used to target these tumors using the HA-binding proteins from cartilage. To test this possibility, we injected a biotinylated form of the cartilage proteoglycan (b-HAbc) into mice that had tumor metastases. We then examined the lungs of this mouse to determine if the b-HAbc had gained access to the HA associated with lung metastases.

6.1. Targeting of lung metastases with b-HAbc: In these studies, we used the α-18 cell line, which is derived from MCF-7 cells that has been transfected with a bacterial *Lac-Z* gene. This allows the tumor to be easily located by staining with X-gal that gives a blue color. These cells have also been transfected with an expression vector for FGF-1 which allows them to metastasize to the lungs (15). These cells were injected into the mammary fat pats of 6-8 week-old nude mice and allowed to grow to form primary tumors of 1-2 gm and at the same time form spontaneous metastases to the lungs. These mice were then given i.v. injections of 200 μg of the b-HAbc. Twenty four hours after the injection, the mice were sacrificed, and the lung tissue was fixed in 3.7% formalin, stained with X-gal and processed for histology.

The histochemical staining showed that in many cases, the metastasis of the α-18 cell were closely associated with the b-HAbc. Thus, it would appear that under the conditions used, the b-HAbc can exit the blood vessels and interact with the HA associated with the tumor cells. Thus, it may indeed be possible to use the HAbc complex to target lung metastases. The complex does appear to be preferentially associated with the α-18 cells present in the lungs. Thus, it may be possible to couple chemotherapeutic agents to the HAbc complex. It is our hope that in the vicinity of the metastasis, this complex this would be taken up by the tumor cells or by the associated macrophages. When the cells degrade the complex in the lysosomes, the chemotherapeutic agent would be released and kill the growing tumor cells. If the

chemotherapeutic agent were cell-cycle dependent, then the tumor cells may be more susceptible than the associated macrophages which are post mitotic.

6.2. Conclusions: The results of these studies suggest that it was possible to target the HA associated with lung metastasis. This possibility was further evaluated in Tasks 7 and 8.

Task 7: To examine the effects of HAbc coupled to MTX on cultured tumor cells: As described above, we believed that drugs attached to the HAbc will bind to the tumor-associated HA and will be taken up by the tumor cells using a CD44 dependent mechanism. To test this possibility, we have examined the ability of HAbc coupled to a chemotherapeutic drug to kill tumor cells in culture. For this experiment, we used methotrexate (MTX), which is widely used as a chemotherapy drug (16, 17).

7.1. Preparation and properties of MTX-HAbc: We prepared a conjugate of MTX and HAbc according to the methods described by Kulkarni (18). When this conjugate was added to cultures of rat fibrosarcoma (RFS) cells, it significantly inhibited their proliferation. Indeed, the activity of the MTX-HAbc was approximately the same as that of equivalent amount of MTX by itself. In general, the when a drug has been coupled to a proteins such as an antibody, it looses its toxicity (19, 20). This is not surprising since the complex must be internalized and degraded by the tumor cell before the coupled drug will be released and exert its activity. Thus, the fact that the complex of MTX-HAbc is active was very encouraging.

7.2. Conclusions: When we initially started these experiments, we thought that the chemotherapeutic drug was necessary for its potential anti-tumor activity. As will be described in the following section, we now know that the HAbc by itself has anti-metastatic activity. For this reason, we concentrated our efforts on further characterizing the effects of the HAbc.

Task. 8. The effect of HA-binding proteins from cartilage on tumor growth: In the course of studying the feasibility of using the HAbc from cartilage to target lung metastases, we decided to test the effect of the HAbc by itself on the formation of experimental metastasis. Initially, these experiments were carried out simply as a control to establish a base line for the HAbc before derivation with the chemotherapeutic agent. Much to our surprise, we found that the HAbc by itself had a sustantial inhibitory effect on the formation of experimental metastases. We were very excited about these results since the HAbc could represent a new avenue for therapeutic intervention. Since these initial observations, we have confirmed and extended the ability of HAbc to inhibit tumor cell growth. More specifically, we now present evidence that the anti-tumor activity is due to the inhibition of angiogenesis, a critical factor in tumor cell growth. These studies will be described in the following sections and were carried out in conjunction with Dr. Shawn Green of EntreMed (Rockville, MD), who played a critical role in their implementation.

8.1. Preparation of the HA-binding complex: For these experiments, the HAbc was isolated from bovine nasal cartilage according to the methods based on those originally described by Tengblad (21). This consisted of briefly treating cartilage extracts with trypsin to reduce the size of the complex and then purifying the HA-binding fraction by affinity chromatography on HA coupled to Sepharose (21, 22). When analyzed by SDS-PAGE (Fig. 3) the final preparation of HAbc consisted of two molecular factions, a diffuse band at approximately 70 to 80 kDa that represents a trypsin fragment of the aggrecan core protein and a sharp band at approximately 38 kDa that corresponds to the link protein. Together these proteins bind to hyaluronan with high affinity and specificity (14). Endotoxin levels in representative

samples of these preparations were consistently low (5 EU/mg protein, the Amebocyte Lysate Test Bio-Whittaker).

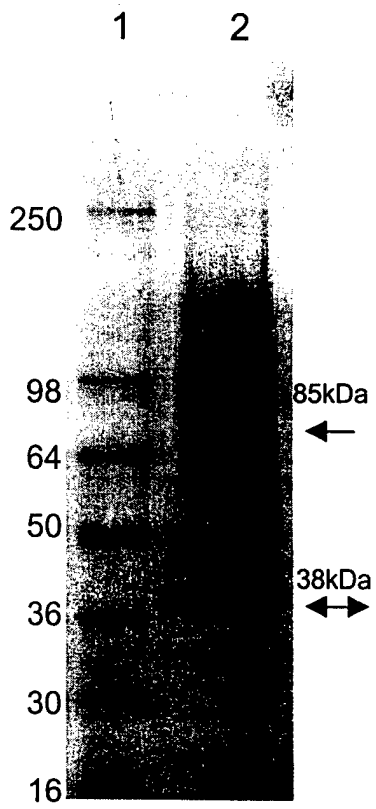

Fig. 3. SDS-PAGE analysis of HAbc. The samples were electrophoresed on a 10% SDS-polyacrylamide gel under non-reducing conditions. Lane 1. Molecular weight standards. Lane 2. The preparation of HAbc shows the trypsin fragment of aggrecan (diffuse band at 85 kDa) and the link protein (38 kDa).

8.2. Mouse Model systems of Metastasis: In initial experiments, we examine the effect of the HAbc on the Lewis lung model of tumor metastasis. For this, three groups of mice were given an i.v. injections of 2 x 10^6 Lewis lung cells on day 0 and beginning on day 3, the mice were given daily i.p. injections of the HAbc complex (0, 15 and 49 μg/injection). Finally, on day 13 the mice were sacrificed and their lungs were removed for examination. Figure 4 shows that the lungs from the control mice (i.e. receiving only saline) had numerous metastases, while those from mice that had been injected with the HAbc complex (49 μg/injection) displayed far fewer metastases. This difference in tumor burden was also reflected by the gross weights of these lungs. Figure 5 shows that the weight of the lungs from the control group was significantly heavier than that of both groups of mice receiving the injections of the HAbc complex. In addition, the higher concentration of HAbc inhibited the growth of the Lewis lung cells to a greater extent than the lower concentration, suggesting that this response shows a dose dependency. Thus, the i.p. injection of the HAbc inhibited the growth of Lewis lung tumor cells in this model system of tumor metastasis.

To determine if a similar response occurred in other tumor cells, we examined B16-BL6 cells that are derived from mouse melanoma cells. In this model system, syngeneic mice were injected i.v. with 5 x 10^4 B16-BL6 cells, and beginning three day later the mice were given daily injections of the various test agents. After 13 days, the mice were sacrificed and the lungs were removed for examination. As shown in Fig. 6, there was an obvious difference between the lungs of mice injected with saline (control) and those injected with the HAbc. However, microscopic examination showed that small tumor nodules were also present in the lungs of the HAbc injected mice. This difference was also apparent when the number of tumor nodules was enumerated. Figure 7 shows that the i.p. injection of the HAbc complex, significantly reduced the number of obvious nodules in a dose dependent fashion, with the $E.D._{50}$ being approximately 10μg per injection. In contrast, the injection of BSA had no discernable effect on the number of metastases. Clearly, the HAbc complex inhibited the growth of the tumor nodules.

Effect of Hyaluronan Binding Protein on Experimental Lung Metastasis (Lewis Lung Cells)

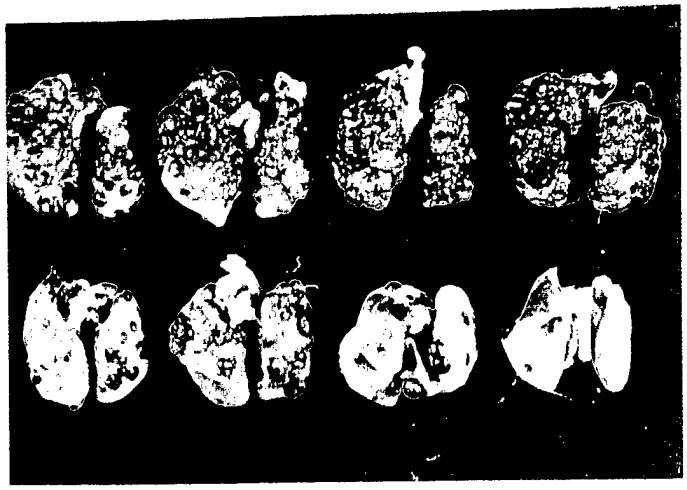

Fig. 4. Lungs from control and HAbc injected mice. The top row shows the lungs from control mice 13 days following the i.v. injection of Lewis lung cells that had received daily injections of saline. Numerous small nodules are apparent on the surface of the lungs. The bottom row shows lungs from mice that had received i.p. injections of the HAbc (49 μg/injection). There is an obvious reduction in the number of tumor nodules on the lungs.

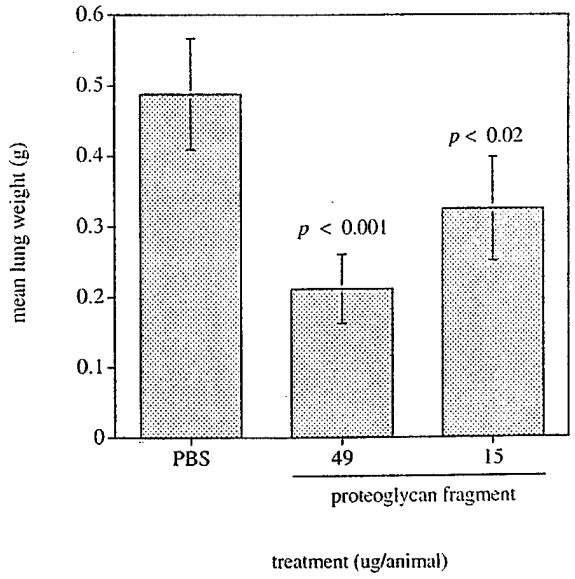

Fig. 5. Weights of lungs from control and HAbc injected mice. The average and standard deviation of the weights from control (saline injected) and HAbc injected mice are shown (n=4 in each group). The HAbc treatment significantly reduced the lung weight, which is a measure of tumor burden. This effect appeared to be dose dependent in that the 49 μg of HAbc per injection was had a greater effect than 15 μg.

Effect of Hyaluronan Binding Protein on Experimental Lung Metastasis (B16 melanoma cells)

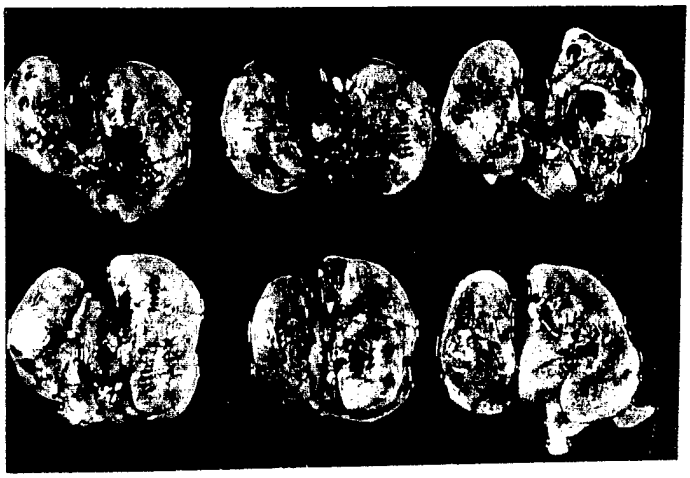

Fig. 6. Tumor nodules of B16BL6 on the lungs from control and HAbc injected mice. The top row shows the lungs of control mice that had been injected i.p. with saline while the bottom row show the lungs of mice that had been injected with the HAbc.

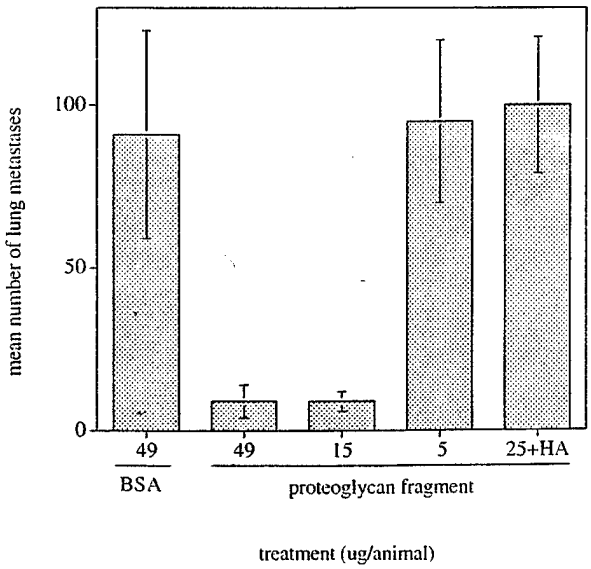

Fig. 7. Bar graph showing the dose response curve of HAbc on number of B16BL6 lung metastases. Compared to an equivalent amount of BSA, the HAbc reduced the number of metastases larger than 0.5 mm.

This phenomenon appears to require the HA-binding activity of the HAbc. As shown in Fig. 7, if the HAbc was first mixed with HA and then injected into the peritoneal cavity of the mice, then the inhibitory effect on the number of lung metastases was abolished. In a similar fashion, if the HAbc preparation was first placed in a boiling water bath prior to the i.p. injections, then the inhibitory effect was blocked (data not shown). These results suggest to us that the ability to bind HA is required for the anti-metastatic activity of the HAbc complex.

8.3. Effect of HAbc on tumor growth in chicken embryos: To determine if the anti-tumor activity of HAbc applied to other model systems, we examined its effect on the growth of xenografts on the chorioallantoic membrane (CAM) of chicken eggs (23). In this model, the tumor cells B16BL6 (mouse melanoma) and TSU (human prostate cancer cells) were applied to the CAMs of 10 day old chicken embryos and allowed to grow for one week. (Note; preliminary studies indicated that none of the mammary carcinoma cells grew in this system). With these two cell lines, the take-rate was almost 100%, giving rise to xenografts of from 50 to 150 mg 7 days after inoculation with one million cells. However, when the inoculated eggs were given a single i.v. injection of the HAbc, then the growth of the B16BL6 and TSU tumor xenografts was greatly inhibited (Fig. 8). This inhibitory effect was abolished if the preparation of HAbc was heat inactivated (Fig. 8 B and D), indicating that the native protein conformation is necessary for the anti-tumor activity. In addition, when the preparation of HAbc was pre-incubated with its ligand HA, the anti-tumor activity was also eliminated (Fig. 8 B), suggesting that that the ability to bind HA is essential for the anti-tumor effect of HAbc. It is important to note that the HAbc did not appear to adversely affect the development of the chicken embryos.

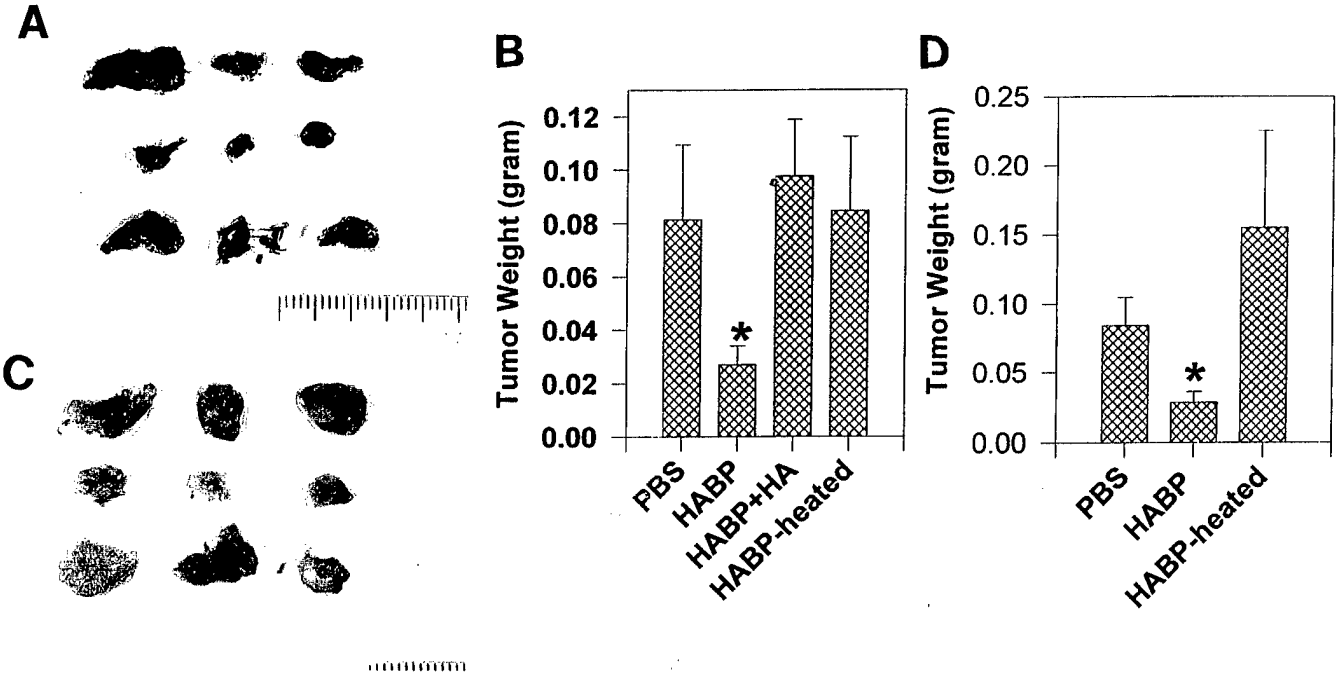

Fig. 8. The effect of HAbc on the growth of tumor cells on the CAMs of chicken embryos. B16BL6 or TSU cells were placed on the CAM of 10 day old chicken embryos and the following day, the eggs were injected i.v. with either native preparations of HAbc or those that had been heat-inactivated or premixed with HA. After 7 days, the xenografts were removed for study. A. Photograph showing the size of B16BL6 xenografts from eggs; top row, saline treatment (control); middle row, after treatment with HAbc; bottom row, heat-inactivated HAbc. B. The weight of the B16BL6 xenografts from eggs after different treatments. C. TSU xenografts; top row, saline treatment (control); middle row, after treatment with HAbc; bottom row, heat-inactivated HAbc. D. The weight of the TSU xenografts.

8.4. Effect of HAbc on growth of cultured cells: The inhibition of tumor cell growth and metastasis by HAbc could be due to either the direct inhibition of tumor cell proliferation or to the disruption of tumor angiogenesis by the host. To distinguish between these possibilities, we examined the effect of HAbc on both cultured endothelial and tumor cells.

Endothelial cells were obtained from three different sources (BREC from bovine retina; ABAE from adult bovine aorta; and HUVEC from human umbilical veins) and were grown on tissue culture dishes in the presence and absence of HAbc. The response of the endothelial cells to the HAbc varied depending upon the cell line. The growth of low passage BREC in anchorage-dependent conditions was strongly inhibited by HAbc in a dose-dependent manner (Fig. 9). Furthermore, this was reversible by heat-inactivation of HAbc and by pre-incubation of HAbc with HA (Fig. 9) In contrast, the HAbc had only a modest inhibitory effect on the growth of the ABAE and the HUVEC cell line (data not showed). Thus, the HAbc appears to block the growth of some, but not all, types of endothelial cells. In particular, the endothelial cells form small blood vessels (BREC) responded to the HAbc to a greater extent than those from larger blood vessels (ABAE and HUVEC).

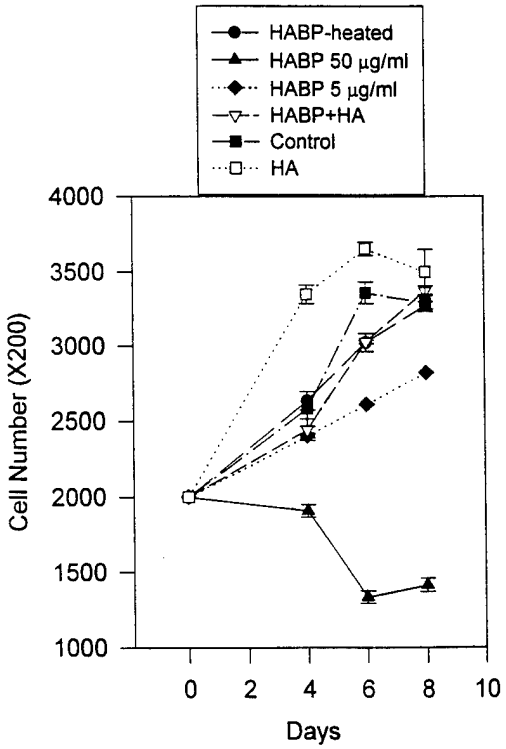

Fig. 9. The effect of HAbc on the growth of cultured BREC cells. The cells were cultured on tissue culture dishes in medium containing 10% fetal calf serum. The medium containing the indicated factors was changed every second day, and the cell number was determined by a Coulter counter.

In the next series of experiments, we examined the effects of HAbc on the growth of tumor cells. When HAbc was added to the culture medium of the tumor cell lines B16BL6, ECV and TSU cells growing in tissue culture dishes, the cell lines exhibited different responses. While the growth of the B16BL6 cells was greatly inhibited by HAbc in a dose-dependent manner by HAbc, the ECV and TSU cells showed little or no response (Fig. 10). These results excluded the possibility of non-specific toxicity of the HAbc preparation and indicated that there was a different susceptibility of tumor cells to HAbc under these growth conditions. The inhibitory effect of HAbc on B16BL6 cells was blocked by both heated-inactivation of the HAbc and by pre-incubation with an excess of HA suggesting, that the effect was specific and required the ability to bind HA.

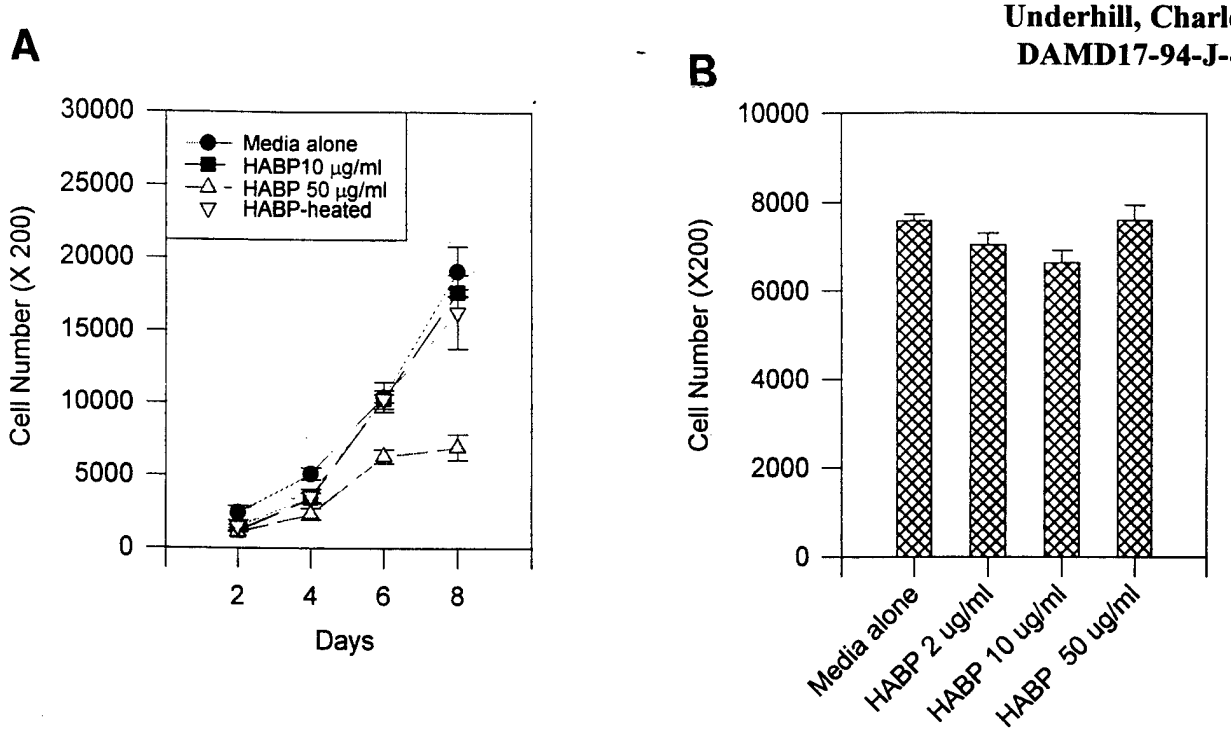

Fig. 10 The effects of HAbc on the growth of tumor cells growing on tissue culture plates. The medium containing the indicated factors was changed ever other day and the cell number was determined with a Coulter counter. A. The growth curve of B16BL6 cells. B. The number of TSU cells after 8 days.

Further experiments revealed that the inhibition of cell growth by HAbc depended upon the specific culture conditions. When HAbc was tested on the growth of tumor cells in soft agar (anchorage-independent conditions), the colony formation of B16BL6 and TSU cells was inhibited (Fig. 11) and this effect appeared to be specific since it was dose dependent (Fig. 11 A), and was reversed by heat inactivation of the HAbc or by premixing with HA (Fig. 11 B). It seems that the inhibitory effect of HAbc in anchorage-independent condition can override the effect that exists in anchorage-dependent condition. It is important to note that anchorage-independent growth in soft agar is one of the best prognostic indicators of whether tumor cells are metastatic *in vivo* (24).

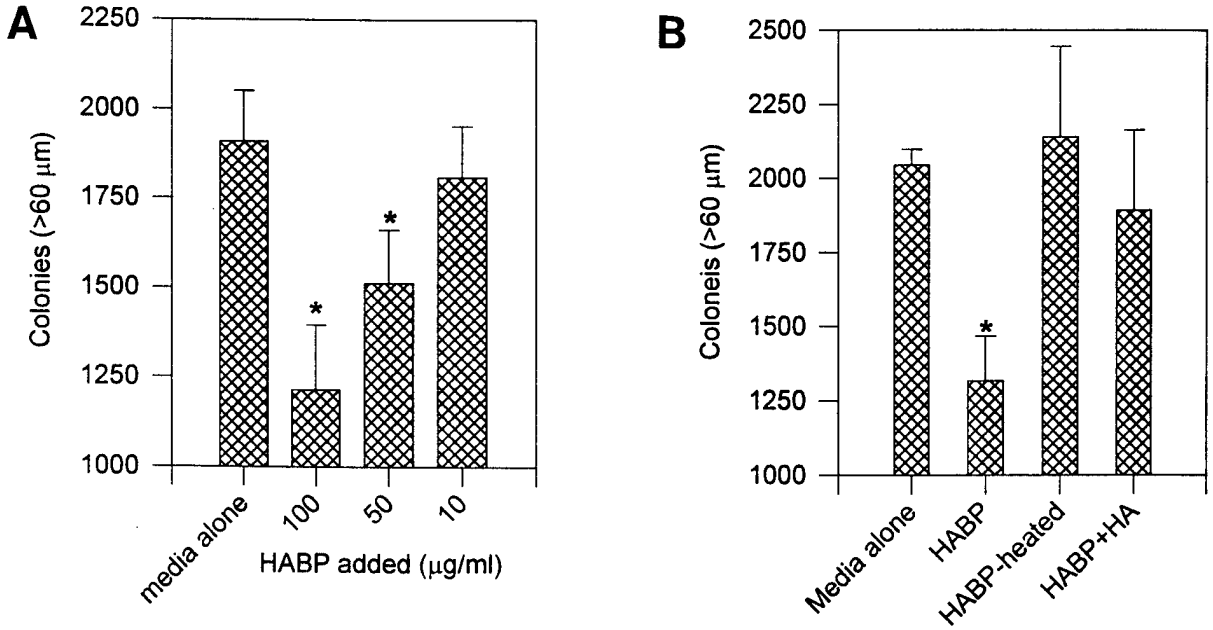

Fig. 11. Effect of HAbc on the cloning efficiency of tumor cells in soft agar. A. The number of clones of B16BL6 cells as a function of HAbc concentration. B. The number of clones of TSU cells.

The differential effects of HAbc on the growth of the various cell lines could be due to different amounts of HA produced by the cells influences the action of HAbc. To explore this possibility we examined the amount of HA secreted by the different cell lines. The conditioned media from B16BL6 and TSU cells were collected after 24 hours and measured for HA concentration by a modified ELISA (22). The results indicated the HA the media from the HAbc sensitive cells (B16BL6 and endothelial cell lines) was much lower than that in the resistant lines (TSU). Thus, it is possible that the free HA in media could bind to HAbc and competitively inhibit its binding to the cell surface and this could account for the differential effects of HAbc.

8.5. Effects of HAbc on apoptosis: Since HAbc inhibited the growth of some endothelial cells and B16BL6 tumor cells, we speculated that it might be inducing apoptosis in these cells. When both BREC and B16BL6 cells were treated with HAbc, a significant increase in DNA fragmentation was observed by Hoechst dye staining at 24 hour (Fig. 12 A). The difference in the fraction of apoptotic cells between the HAbc treated group and the control groups was quite significant at 72 hours after treatment (Fig. 12 A). The HAbc induced apoptosis was also confirmed by DNA fragment analysis with flow cytometry. The percentage of the cells with fragmented DNA fragment was significantly increased in both endothelial cells (3% vs. 11-12%) and B16BL6 cells following treatment with HAbc (Fig. 12 B). These results strongly suggest that HAbc induces apoptosis and this is responsible for its inhibitory effects on angiogenesis and tumor growth. However, at this point, the mechanism by which HAbc triggers programmed cell death is unclear.

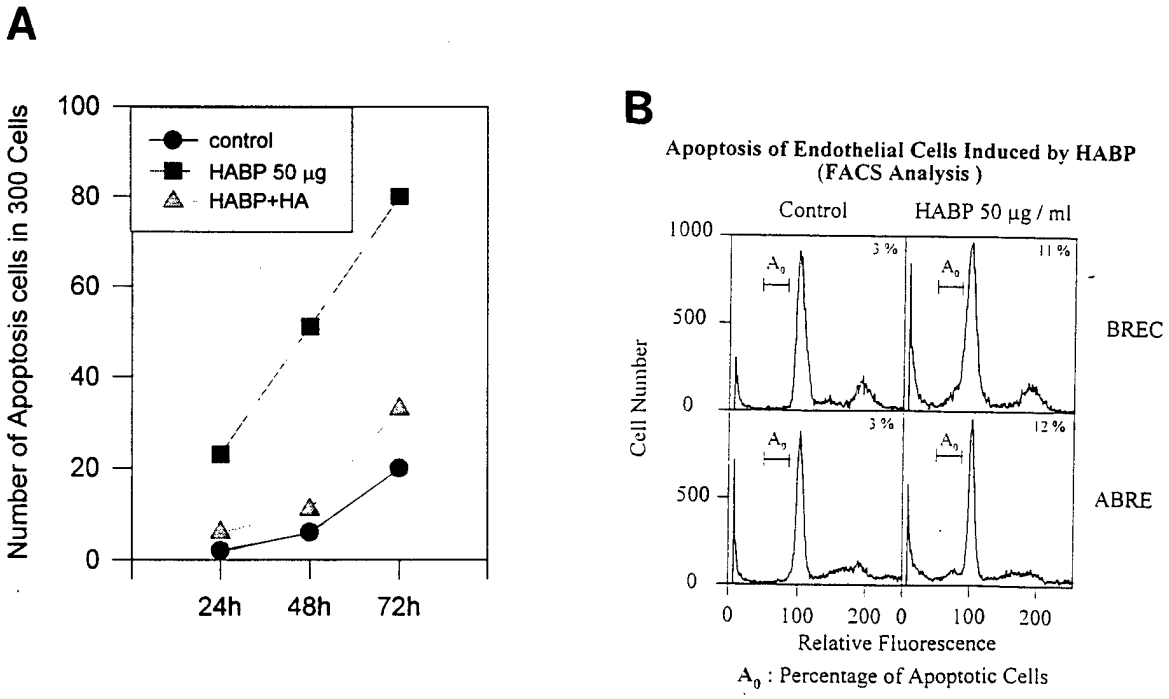

Fig. 12. The effects of HAbc on the rate of apoptosis in tumor and endothelial cells. A. The fraction of B16BL6 cells demonstrating nuclear fragmentation by staining with Hoechst dye is shown. Similar effects were obtained with the endothelial cells. B. Analysis of DNA fragmentation in endothelial cells (BREC and ABAE) by flow cytometry. Similar results were obtained with B16BL6 cells.

8.6. Effects of HAbc on angiogenesis in the chicken CAM: To determine if HAbc could directly block angiogenesis *in vivo*, we examined its effect on the chick CAM assay (28). For this, filter papers were saturated recombinant human VEGF and placed on the CAMs of 10 day old eggs. The test group was given a single i.v. injection of HAbc while the control groups received either saline vehicle alone or heat-inactivated HAbc. Three days later, the extent of vascularization in the region of the filters was determined by computerized assisted image analysis. The results showed that both length and area of vessels in HAbc treated were greatly reduced compared to the control groups (Fig. 13), suggesting that HAbc does indeed have the ability to block angiogenesis.

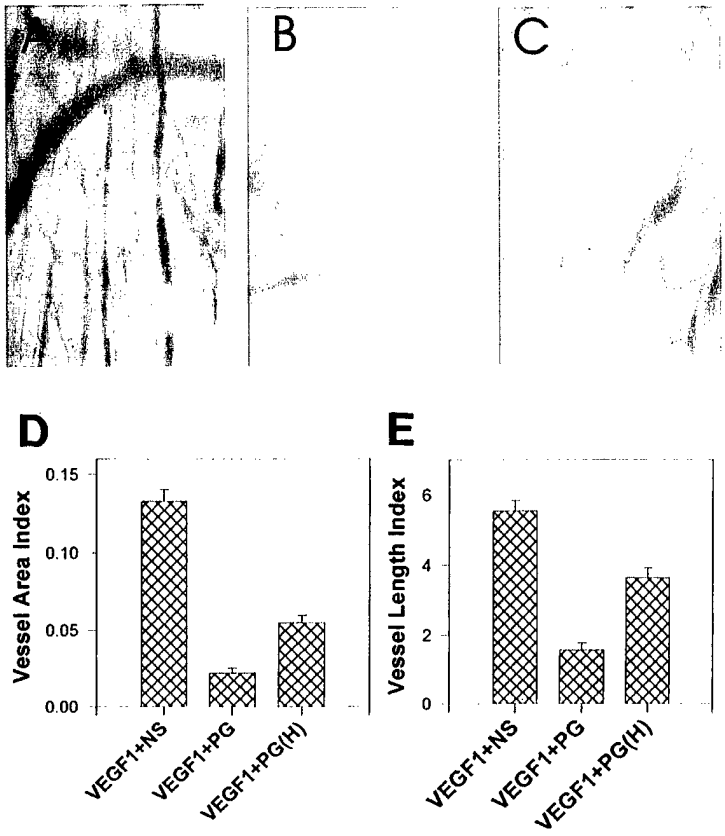

Fig. 13. The effects of HAbc on VEGF induced angiogenesis in the chicken CAM. This assay was performed according to the methods of Brooks et al. with some modifications (23). The top air sac portions of 10-day-old chicken eggs were opened, the CAMs exposed and filter disks (0.5 cm diameter) containing 15 ng VEGF were applied to the CAMs. The CAMs were then injected with the various agents (80 μg/egg) and on day 3, the CAMs and associated discs were cut out and analyzed. A. Blood vessels from a CAM of embryos injected with saline. B. Blood vessels of a CAM from an embryo that had been injected with HAbc. C. Blood vessels from a CAM of an embryo injected with HAbc that had been heat-inactivated. D. and E. Computer analysis of the blood vessel indices are shown. For this analysis, the discs were divided into 4 quarters with fine wires. The blood vessels in each quarter of the CAM were digitally photographed and the results were analyzed by an Optimas 5 program to calculate the vessel area and length in the viewing area. The total length and area of the vessels in the 4 quadrants of each disc were normalized to the total area measured and expressed as vessel length or area index.

8.7. Conclusions: Based upon the results of this study, we believe that the anti-tumor activity of HAbc is due to the inhibition of tumor angiogenesis. More specifically, following injection, the HAbc circulates in the blood and binds to HA on the endothelial cells that are involved in the neovascularization of tumors. This interaction leads to the induction of the apoptotic cascade in these cells causing their death and thereby blocking further angiogenesis.

While far from being proven, this hypothesis is consistent with most of our data. Our observation that the anti-tumor activity of HAbc was blocked by pre-incubating it with exogenous HA strongly suggests that HA is the ligand against which the HAbc is directed. It is important to note that under normal physiological conditions, the levels of HA in the blood are maintained at very low levels by the liver and lymphatic system even though there are high levels present in the connective tissue (27, 28). Thus, the circulating HAbc should retain its HA binding activity.

The fact that HAbc is able to able to inhibit VEGF-induced angiogenesis in the chicken CAM system suggests that it can act directly on endothelial cells of newly forming blood vessels. This is reasonable in view of earlier studies by Ausperdunk *et al.* showing that HA is localized the tips of newly forming capillaries in the chicken CAM (25). In addition, Mohamadzadeh *et al.* has found that the synthesis of HA by endothelial cells was stimulated by pro-inflammatory cytokines (26). Interestingly, this stimulation was restricted to endothelial cells derived from the small blood vessels but not larger ones. Perhaps this could account for our observation that HAbc specifically inhibited the growth of endothelial cells from small blood vessels as opposed to those from larger ones (BREC vs. ABAE and HUVEC cells, see section 8.4.). Thus, HA appears to specifically associated with the endothelial cells of newly forming blood vessels.

The question still remains as to how the HAbc becomes associated with the targeted cells to exert its inhibitory effects. One possibility is that the endothelial cells take up the HA as well as any bound HAbc into an endosomal compartment where the HAbc becomes active. This is consistent with the observations of Banerjee and Toole as well as Griffioen *et al.* that activated endothelial cells express receptors for HA including CD44 (29, 30). In earlier studies, we had shown that CD44 plays a critical role in the uptake and degradation of HA by a variety of cell types (3, 4). The CD44 allows cells to bind to HA so that it can be internalized into endosomal compartments where the HA is degraded. Thus, the expression of CD44 by the endothelial cells may allow them to internalize the HA and any associated HAbc. However, how this event could lead to the induction of apoptosis in the targeted cells is unresolved and clearly needs to be addressed in future studies.

While we believe that the HAbc is acting against endothelial cells, it is also possible that it is also acting directly against the tumor cells themselves. Indeed, we did find that the HAbc could inhibit the growth of B16BL6 and TSU cells in culture. A recent study by Hendrix *et al.* has indicated that some tumors including melanomas have the ability to form vasculature independent of endothelial cells (31). The tumor cells themselves appear to take on the characteristics of endothelial cells and are responsible for the formation of blood vessels. It is possible that such tumor cells could also respond to the HAbc.

In summary, we have found that HAbc is able to block tumor growth under a variety of conditions, and this effect depends upon the ability of the complex to bind HA. The most likely explanation is that the HAbc is targeting endothelial cells that are involved in the neovascularization of tumors, although the tumor cells themselves may also be targeted. It is also important to note that the HAbc did not have any obvious deleterious effect on either the mice or the chicken embryos.

It is our hope that the effects of HAbc represent a novel mechanism for inhibition of tumor growth that may lead to the design of new therapeutic approaches for the treatment of cancer. Clearly, there are a number of issues concerning the anti-tumor activity of HAbc that need to be resolved. First, what is the minimum size of the complex that is required for activity? Secondly, how does it induce apoptosis in endothelial or other targeted cells. And third, is it active against a wide spectrum of tumor types or only against a specific subset.

ACRONYMS AND SYMBOL DEFINITIONS

b-HAbc	Biotinylated proteoglycan - used as specific staining probe for hyaluronan.
CAM	Chorioallantoic membrane
CD44	Cluster of determination (differentiation) - same as the hyaluronan receptor or binding site.
CMF-PBS	Calcium and magnesium free phosphate buffered saline.
DMEM	Dulbecco's modifed Eagle's medium
HA	Hyaluronan.
HAase	Hyaluronidase (either testicular or *Streptomyces*)
KM-201	Rat monoclonal antibody directed against mouse CD44
mAb	Monoclonal antibody.
MTX	Methotrexate, a cell-cycle dependent chemotherapeutic agent.
MTX-HAbc	A derivative of MTX coupled to the HAbc.
HAbc	A complex of a trypsin fragment of cartilage proteoglycan and link protein that binds to HA with high affinity and specificity.
RFS	Rat fibrosarcoma cell line that express large amounts of HA on its surface.
SDS-PAGE	Sodium dodecyl sulfate polyacrylamide gel electrophoresis.
SV-3T3	Simian virus 40 transformed mouse 3T3 cells (Swiss mouse).

KEY RESEARCH ACCOMPLISHMENTS:

- Both primary and secondary tumors of breast cancer are heterogeneous with respect to the expression of CD44. There does not appear to be a close correlation between the expression of CD44 and the formation of metastases.
- Treatment with HAase stimulated the growth of Bi1BL6 tumor cells on the CAMs of chicken embryos. This effect is probably due to an increase in number of blood vessels in the center of the tumor. This suggests that HA does play a role in vascularization.
- In general, there is an inverse correlation between the expression of CD44 and the presence of HA. Presumably, this is due to the fact that CD44 allows cells to take up and degrade HA. However, exceptions to this were noted in several cases. It is possible that in these regions, the extent of HA synthesis was so great, that the CD44 mediated degradation was not sufficient to remove all of it.
- The presence of HA did not appear to be directly correlated with the distribution of endothelial cells (blood vessels) in biopsies of human breast cancer.
- Large amounts of HA were associated with tumors that have metastasize to the lungs. This phenomenon may be useful for targeting agents to the tumors.
- When b-HAbc was injected into mice, it can become preferentially associated with tumor metastases present in the lungs.
- A complex consisting of MTX coupled to HAbc is active in blocking the proliferation of tumor cells in culture.
- HAbc by itself was able to inhibit the formation of lung metastases in mice and the growth of tumor cells on the CAM of chicken embryos. However, it did not appear to have any deleterious effects on the host mice or chicken embryos. HAbc could also block the growth of some types of tumors and endothelial cells in tissue culture.
- HAbc was able to block the VEGF-induced angiogenesis of the chicken CAM, suggesting that its anti-tumor activity may be due to its ability to inhibit vascularization of tumors.

REPORTABLE OUTCOMES:

Manuscripts (acknowledging support from this grant):

Underhill, C. B. and Zhang, L. 1999. Analysis of Hyaluronan using biotinylated hyaluronan-binding proteins. in *Methods in Molecular Biology*. **137** in press

Zeqiu H, Ni, J., Smits, P., Underhill, C. B., Xie, B., Liu, N., Tylzanowski, P., Parmelee, D., Feng, P., Ding, I., Gao, F., Gentz, R., Huylebroeck, D., Merregaert, J. and Zhang, L. 1999 Extracellular matrix protein 1 (ECM1) is an angiogenic factor expressed by breast tumor cells. Submitted.

Liu, N., Underhill, C. B., Lapevich. R. K., Han, Z., Gao, F., Zhang, L and Green, S. J. 1999. Tumor Growth Inhibition by a Hyaluronan Binding Complex From Cartilage (Metastatin). to be submitted.

Patents and licenses applied for:

Anti-tumor activity of a Hyaluronan-binding complex from cartilage
Charles Underhill and Shawn Green.

CONCLUSION AND SIGNIFICANCE:

- The major significance of this research is that we have identified a new anti-tumor reagent, namely HAbc. We have presented evidence that the anti-tumor activity of the HAbc is due to its ability to induce apoptosis in endothelial cells that, in turn, inhibits tumor vascularization and growth. It is possible that this complex could prove useful in a clinical setting in the fight against cancer. On the other hand, even if HAbc itself is not suitable for use in cancer patients, the further study of its anti-tumor activity could lead to the development of other reagents that are appropriate. In either case, this complex deserves further investigation.

REFERENCES:

1. Laurent ,T. C. 1987. Biochemistry of hyaluronan. Acta Otolaryngol; **442**: 7-24
2. Toole , B. P.: Glycosaminoglycans in morphogenesis. In cell *Biology of the Extracellular Matrix*, Hay E. D., ed. New York: Plenum Press, PP259-294.
3. Culty, M., Nguyen, H. A., and Underhill, C. B. 1992. The hyaluronan receptor (CD44) participates in the uptake and degradation of hyaluronan. *J. Cell Biol.*, **116**:1055-1062.
4. Culty, M., Shizari, M., Thompson, E.W., and Underhill, C.B. 1994 Binding and degradation of hyaluronan by hyman breast cancer cell lines expressing different froms of CD44: Correlation with invasive potential. *J. Cell Physiol.* 160: 275-286.
5. Underhill, C. B. 1992. CD44: The Hyaluronan Receptor. *J. Cell Sci.* **103**: 293-298
6. Guy, C. T., R. D. Cardiff and W. J. Muller. 1992. Induction of mammary tumors by expression of polyomavirus middle T oncogene: A transgenic mouse model for metastatic disease. *Molec. Cell. Biol.* **12:**954-961.
7. Kusakabe M, Skakura T, Nishizuka Y, Sano M, Matsukage A: 1984. Polyester wax embedding and sectioning technique for immunohistochemistry. *Stain Technol* **59**:127-132
8. Mantovani, A., Ming, W. J., Balotta, C., Abdeljalil, B., and Bottazzi, B. 1986. Origin and regulation of tumor-associated macrophages: the role ot tumor-derived chemotractic factor. *Biochem. Biophys. Acta* **865**: 59-67
9. Brunda, M. J., Sulich, V., Wright, R. B. and Palleroni, A. V. 1991. Tumoricidal activity and cytoking secretion by tumor-infiltrating macrophages. *Int. J. Cancer* **48**:704-708.
10. Nettelbaladt, O., Beergh, J., Schenholm, M., Tengblad, A., Halgren, R. 1989. Accumulation of hyaluronic acid in the alveolar intersitial tissue in bleomycin-induced alveolitis. *Am. Rev. Respir. Dis.* **139**: 759-762
11. Sahu, S. 1980. Hyaluronic acid - an indicator of the pathological conditions of human lungs. *Inflammation* **4**: 107-112
12. Sahu, S.C. and Ulsamer, A.G. 1980. Hyaluronic acid - an indicator of pulmonary injury? *Toxicol. Lett.* **5**: 283-286.
13. Green, S.J., Tarone, G. and Underhill, C.B. 1988 Aggregation of macrophages and fibroblasts is inhibited by a monoclonal antibody to the hyaluronate receptor. *Exp. Cell Res.* 178: 224-232
14. Green, S.J., G. Tarone, and C. B. Underhill. 1988. Distribution of hyaluronate and hyaluronate receptors in the adult lung. *J. Cell Sci.* **89:**145-156.
15. Zhang, L., Ding, I. Y. F., Kharbanda, S., Chen, D. Mcleskey, S. W., Honig, S., Kern, F. G.: 1997. MCF-7 breast carcinoma cells overexpressing FGF-1 form vascularized, metastatic tumors in ovariectomized and tamoxifen-treated nude mice. *Cancer Res.* in press
16. Johns , D.G., and Bertino, J. R.: Folate antagonist. In: Holland, J. F. and Frei, E., (eds). *Cancer Medicine*. Philadelphia: Lea and Febiger 1973; pp 739-754
17. Salmon, S. and Sartorelli, A. C. 1992. Cancer chemotherapy in Basic and Clinical Pharmacology Katzung, 5th edition, B. G. ed. Prentice Hall, Conneticut, pp. 766-800
18. Kulkarni, P. N., Blair, A. H., and Ghose, T.: 1981. Covalent binding of methotrexate to immunoglobulins and the effect of antibody-linked drug on tumor growth in vivo. *Cancer Res.* **41**: 2700-2706.
19. Kanelloes, J., Pietersz, G. A., and McKenzie, I. F.C.: 1985. Studies of methotrexate-monoclonal antibody conjugates for immunotherapy. *JNCI* **75**: 319-332.
20. Fritzpatrick, J. J. and Garnett, M. C. 1995. Studies on the mechanism of action of an MTX-HSA-MoAB conjugate. *Anti-canc Drug Design* **10**:11-24
21. Tengblad, A. 1979. Affinity chromatography on immobilized hyaluronate and its application to the isolation of hyaluronate binding proteins from cartilage. *Biochim. Phiohys. Acta*, **578**:281-289

22. Underhill, C. B. and Zhang, L. 1999. Analysis of Hyaluronan using biotinylated hyaluronan-binding proteins. in *Methods in Molecular Biology*. **137** in press
23. Brooks, P. C., Silletti, S., von Schalscha, T. L., Friedlander, M., and Cheresh, D. A. 1998. Disruption of angiogenesis by PEX, a noncatalytic metalloproteinase fragment with integrin binding activity. *Cell* **92:** 391-400
24. Shin, S.-S., Greedman, V. H., Risser, R. and Pollack, R. 1975. Tumorigenicity of virus-transformed cells in nude mice is correlated specifically with anchorage independent growth in vitro. *Proc. Natl. Acad. Sci. USA* **72**: 4435-
25. Ausprunk, D. H. 1986. Distribution of hyaluronic acid and sulfated glycosaminoglycans during blood-vessel development in the chick chorioallantoic membrane. *Amer. J. Anat.* **177**:313-331.
26. Mohamadzadeh M. DeGrendele, H., Arizpe, H., Estess, P., and Siegelman, M. 1998. Proinflammatory stimuli regulate endothelial hyaluronan expression and CD44/HA-dependent primary adhesion. *J. Clin. Invest.* **101:** 97-108
27. Laurent, T. C. Fraser, J. R. E. Pertoft, H., and Smedsrod. 1986. Binding of hyaluronate and chondroitin sulphate to the liver endothelial cells. *Biochem. J.* **234**:653-658
28. Fraser, J. R. E. Appelgren, L. E., Laurent, T. C. 1983. Tissue uptake of circulating hyaluronic acid. *Cell Tissue Res.* **233**:285-293
29. Banerjee, S. D. and Toole, B. P. 1992. Hyaluronan-binding protein in endothelial cell morphogenesis. *J. Cell Biol.* **119**:643-652.
30. Griffioen, J. W., Goenen, M J.H. Damen, C. A., Hellwzig, S. M. M. wan Weering, D. H. J. Vooys, W., Blijham, G. H. and Groenewegn G. 1997. CD44 is involved in tumor angiogenesis; an activation antigen on human endothelial cells. *Blood.* **90**:1150-1159
31. Maniotis A. J. Folber, R., Hess, A., Seftor, E. A., Gardner, L. M. G., Pe'er, J. Trent, J. M. Meltzer, P. S. and Hendrix, M. J. 1999. Vascular channel formation by human melanoma cells in vivo and in vitro: Wasculogenic mimicry. *Am J Pathol.* **155**:739-752

FINAL REPORT

Bibliography

Underhill, C. B. and Zhang, L. 1999. Analysis of Hyaluronan using biotinylated hyaluronan-binding proteins. in *Methods in Molecular Biology*. **137** in press

Zeqiu H, Ni, J., Smits, P., Underhill, C. B., Xie, B., Liu, N., Tylzanowski, P., Parmelee, D., Feng, P., Ding, I., Gao, F., Gentz, R., Huylebroeck, D., Merregaert, J. and Zhang, L. 1999 Extracellular matrix protein 1 (ECM1) is an angiogenic factor expressed by breast tumor cells. Submitted.

Liu, N., Underhill, C. B., Lapevich. R. K., Han, Z., Gao, F., Zhang, L and Green, S. J. 1999. Tumor Growth Inhibition by a Hyaluronan Binding Complex From Cartilage (Metastatin). to be submitted.

List of personnel

1. Underhill, Charles B.
2. Culty, Martine
3. Swartz, Ronald
4. Zhang, Lurong

Article to PNAS

Classification: Biological Sciences: Cell Biology

EXTRACELLULAR MATRIX PROTEIN 1 (ECM1) IS AN ANGIOGENIC FACTOR EXPRESSED BY BREAST TUMOR CELLS

Zeqiu Han[1], Jian Ni[2], Patrick Smits[4], Charles B. Underhill[1], Bin Xie[1], Ningfei Liu[1], Przemko Tylzanowski[5], David Parmelee[2], Ping Feng[2], Ivan Ding[3], Feng Gao[1], Reiner Gentz[2], Danny Huylebroeck[5], Jozef Merregaert[4] and Lurong Zhang[1]

[1]Department of Cell Biology, Georgetown University Medical Center, 3900 Reservoir Road, NW, Washington DC 20007; [2] Human Genome Sciences, Inc., 9410 Key West Avenue, Rockville, MD 20850; [3] Department of Radiology, Rochester University Medical Center, Rochester, NY 14642;[4] Laboratory of Molecular Biotechnology, Department of Biochemistry, Universiteitsplein1, B-2610 Wilrijk, Belgium. [5] Laboratory of Molecular Biology (Celgen) and Department of Cell Growth, Differentiation and Development (VIB-07) Flanders Interuniversity Institute of Biotechnology (VIB), University of Leuven, Herestraat 49, B- 3000 Leuven, Belgium.

Zeqiu Han, Jian Ni and Patrick Smits share first authorship

Jozef Merregaert and Lurong Zhang share senior authorship.

Corresponding author: Lurong Zhang, Department of Cell Biology, Georgetown University Medical Center, 3900 Reservoir Road, NW, Washington DC 20007; Tel: 202-687-6397; FAX: 202-687-1823; E-mail: Zhangl@gusun.georgetown.edu

Manuscript information: 20 pages of text; 7 pages of figures

Word and character counts: 187 words in abstract; total 47,000 characters

ABSTRACT

Tumor growth and metastasis depends critically upon the formation of new blood vessels. In the present study, the extracellular matrix protein 1 (ECM1), a newly described secretory glycoprotein, was found to promote angiogenesis. This was initially suggested by *in situ* hybridization studies of mouse embryos indicating that ECM1 message was associated with blood vessels and its expression pattern was similar to flk-1, a recognized marker for endothelium. Furthermore, ECM1 could also bind to heparin and hyaluronan in a dose-dependent manner, a property shared by other angiogenic factors. More direct evidence for ECM1's role in angiogenesis came from the observation that highly-purified recombinant ECM1 stimulated the proliferation of cultured endothelial cells and promoted blood vessel formation in the chorioallantoic membrane of chicken embryos. Immunohistochemical staining with specific antibodies indicated that ECM1 was expressed by the human breast cancer cell lines MDA435 and LCC15 that are highly tumorigenic. In addition, ECM1 was detected in a significant proportion of primary and secondary tumors in tissue sections from patients with breast cancer. Collectively, the results of this study suggest that ECM1 is an angiogenic factor that may promote tumor progression.

INTRODUCTION

Angiogenesis represents a critical factor in tumor progression (ref). Prior to the formation of blood vessels, most tumors are relatively small, remain localized and grow at a slow rate. However, with the advent of vascularization, these *in situ* tumors are transformed into a more malignant phenotype characterized by rapid growth, invasiveness and metastasis. In many cases, tumor cells facilitate their own progression by directly producing angiogenic factors such as vascular endothelium growth factor (VEGF) and fibroblast growth factors (FGFs), to stimulate a persistent angiogenesis that leads to their uncontrolled growth and metastasis. Alternatively, some tumors act by inducing the normal cells to synthesize the angiogenic factors[13-15, 22]. In either case, the process of neo-vascularization represents a common feature of malignant progression of solid tumors and as such represents a potential target to inhibit tumor growth and metastasis.

In this study, we have examined the angiogenic properties of the extracellular matrix protein 1 (ECM1) that was initially isolated from an osteogenic stromal cell line[1, 2]. Earlier sequencing studies indicated that while ECM1 is not directly homologous to any other know protein, it does contain CC-(X_{7-10})-C motifs, similar to those in serum albumin [3, 4]. Such sequences potentially generate "double-loop" domains that are likely involved in interactions with other proteins[5, 6]. In humans, the ECM1 message is differentially spliced, giving rise to two forms of the protein; a long form (ECM1a) composed of 540 amino acids; and a short form (ECM1b) of 415 amino acids that lacks the amino acids derived from the central seventh exon[2]. Northern analysis of different human tissues has indicated that the 1.8 kb transcript for ECM1a was expressed predominantly in the blood vessel rich placenta and heart, while the 1.4 kb mRNA for ECM1b was present in the tonsils and skin[2, 4].

Previous studies have suggested that ECM1a plays a regulatory role in the process of endochondral bone formation (Deckers *et al.*, submitted for publication). In the mouse embryo, Ecm1a mRNA was expressed by perichondral connective tissue but not by the chondrocytes. Furthermore, when

recombinant human ECM1a was added to organ cultures of metatarsals isolated from mouse embryos, it modulated both alkaline phosphatase activity and mineralization in a dose-dependent fashion. Thus, ECM1a produced by perichondral tissue appears to act in a paracrine fashion to alter the behavior of chondrocytes in the embryo. However, beyond this, little was known about other possible functions of ECM1.

Here, we report that ECM1 also possesses angiogenic-promoting properties as suggested by its close association with embryonic and extra-embryonic angiogenesis, and its stimulatory effect on endothelial cell proliferation both *in vitro* and *in vivo*. Furthermore, the fact that ECM1 is up-regulated in some breast cancer cells suggests that it may play a role in tumor progression.

MATERIALS AND METHODS

Mouse Ecm1 probe and *in situ* hybridization. The pUIA671 construct used for the *in situ* hybridization was made by ligating a 512 bp *Pst I* fragment of the 5' region of mouse ECM1 cDNA into the *Pst I* cloning site of pSport (Life Technologies, Gaithersburg, MD). *In situ* hybridization was done as previously described[23].

Expression and purification of human ECM1. The human cDNA sequences encoding ECM1a and ECM1b proteins were amplified by PCR using human fetal liver cDNA library as template and the following primers: 5'-primer 5'-CGGGATCCGCCATCATGGGGACCACAGCCAG-3', consisting of a *BamH I* restriction site, a "Kozak" sequence and the first 17 bases of the open reading frame; 3'-primer 5'-GCTCTAGATCCAAGAGGTGTTTAGTG-3', containing a *Xba I* restriction site followed by 18 nucleotides complementary to the 3' untranslated sequence. The amplified fragments were cloned into the baculovirus expression vector pA2. The generation of recombinant baculoviruses and expression of ECM1 were performed as described previously[24, 25].

For isolation of the ECM1a protein, conditioned media from the virus-infected insect cells was directly applied to a strong cation-exchange column (Poros HS, PerSeptive Biosystems) equilibrated with 0.05 M NaCl, 0.02 M Bis-Tris, pH 6.0, and 10% (v/v) glycerol (Buffer A). The protein was eluted with a step gradient of a high ionic strength buffer consisting of 35% 1.0 M NaCl, 0.02 M Bis-Tris, pH 6.0, and 10% (v/v) glycerol (Buffer B). The fractions containing protein were pooled and diluted with water to reduce the ionic strength. The sample was clarified by centrifugation, and then applied to a strong anion-exchange column (Poros HQ) connected in tandem to a strong cation-exchange column (Poros HS) pre-equilibrated with Buffer A. The columns were eluted with a gradient from 0 to 70% Buffer B. The fractions containing ECM1a, as determined by SDS-PAGE, were pooled, diluted with water and adjusted to pH 8.0 with 0.5 M Bis-Tris propane (pH 9.0). The resulting solution was then applied to a Poros HQ

column equilibrated with Buffer A at pH 8.0. The proteins were eluted using a gradient of from 0 to 100% Buffer B at pH 8.0.

The ECM1b was purified in a similar fashion with only slight modification of the buffers. For the first cation-exchange column (Poros HS), the proteins were eluted with a step gradient of 35% 2.0 M NaCl, 0.02 M Bis-Tris, pH 6.0, and 10% (v/v) glycerol (Buffer C). The ECM1b containing peaks were pooled, diluted and adjusted to pH 8.0. For the second columns (Poros HS and HQ connected in tandem), the proteins were eluted with a gradient of from 0 to 50% 2.0 M NaCl, 0.02 M Tris pH 8.0. For the final purification step, the fractions containing ECM1b, were pooled, diluted and adjusted to pH 5.0, applied to an HS column, and eluted with a gradient from 0-100% Buffer C.

The fractions containing purified ECM1a or ECM1b were analyzed by SDS-PAGE and those containing a single band were pooled. The identity of these preparations was verified by N-terminal amino acid sequencing and the purity was found to be greater than 98% pure by RP-HPLC analysis. Endotoxin levels of the preparations were less than 5 EU/mg protein as determined by the Amebocyte Lysate Test (Bio-Whittaker).

Preparation of antisera. Antibodies against human ECM1 were raised by injecting 0.2 mg of highly-purified recombinant ECM1a or Ecm1b in Freund's complete adjuvant (Difco Laboratories) subcutaneously into rabbits. The injections were repeated after three weeks and the rabbits were bled every third week. While the antiserum generated by immunization with ECM1a cross-reacted with ECM1b and vice versa, they were specific for ECM1 as determined by ELISA and immuno-electrophoresis using the recombinant proteins. In some cases, the antibodies were further purified by affinity chromatography on ECM1 coupled to Sepharose 4B.

Cell culture and sources of tissues and materials: The human breast cancer cell lines (MCF-7, Hs578T, MDA-468, MDA-435, Sk-Br-3, ZR571, and T47D) were purchased from ATCC (Rockville, MD). The LCC-15 (derived from a bone metastasis of breast cancer patient), the human umbilical vein endothelial cells (HUVEC) and the primary as well as metastatic breast cancer tissues were obtained from

the Tumor Bank of the Lombardi Cancer Center, Georgetown University. Adult bovine aorta endothelial cells (ABAE) were kindly provided by Dr. Luyuan Li (Lombardi Cancer Center) and the bovine retinal endothelial cells (BREC) by Dr. Higger (Dept. of Pediatrics, Georgetown University Hospital). The tumor cells were maintained in 5% fetal bovine serum, 95% DMEM and the endothelial cells in 10% fetal bovine serum, 90% DMEM containing 10 ng/ml basic FGF. All the cells were cultured in a humidified 5% CO_2 incubator at 37°C. Heparin was purchased from Sigma (St. Louis, MO), HA from Lifecore Science (Minneapolis, MN), heparin-Sepharose 4B from Pharmacia (Piscataway, NJ) and HA-Sepharose 6B was prepared according to the methods of Tengblad[26].

ELISA assays: Heparin (20 U/ml) or HA (400 μg/ml, Sigma) in PBS was applied to Probind plates (Falcon, Franklin Lakes, NJ) and incubated overnight at 4°C. The plates were blocked with 10% calf serum, 90% PBS and 0.1% Tween 20, and then varying concentrations of ECM1a and ECM1b with or without pre-incubation with 30 μg of HA or 20 U of heparin were added to the wells and incubated for 1 hour at room temperature. The wells were incubated sequentially with: 1) rabbit anti-ECM1a or anti-ECM1b (1:1,000); 2) peroxidase conjugated anti-rabbit antibody (1:2,000); and 3) the peroxidase substrate azinobis (3-ethyl-benzthiazoline sulfonic acid) and H_2O_2. The A_{405} was then recorded with an ELISA plate-reader.

To detect binding of HA to immobilized ECM1, human recombinant ECM1a (10 μg/ml) was coated on the surface of a Probind plate, which was sequentially incubated with: 1) serial dilutions of HA; 2) 4 μg/ml of biotinylated HA binding protein (b-PG)[26] diluted in PBS; 3) peroxidase labeled-streptavidin; and 4) azinobis (3-ethyl-benzthiazoline sulfonic acid) and H_2O_2. The results were read in an ELISA plate-reader at A_{405}.

Interactions of ECM1 with heparin and HA. Soluble ECM1 (1 or 5 μg) was added to 100 μl of a 30% suspension of heparin-Sepharose 4B or HA-Sepharose 6B with or without preincubation with soluble heparin (100 U) or HA (100 μg). After washing, the bound ECM1 was disassociated with 30 μl of Laemmli sample buffer, separated by electrophoresis on a 10% SDS-polyacrylamide gel, transferred to

a nitrocellulose membrane and detected with rabbit anti-ECM1a or anti-ECM1b (1:1,000) and peroxidase labeled anti-rabbit antibodies (1:4,000) followed by ECL (Amersham, Buckinghamshire England).

Effect of ECM1 on proliferation of endothelial and tumor cells: The endothelial cells and the MDA435 and MDA468 tumor cells were subcultured into 96 well plates, maintained in serum-free media for 24 hours and then incubated with 5, 20, 50 or 100 ng/ml of ECM1a in 1% fetal bovine serum, 99% DMEM. Twenty four hours later, the proliferation of cells was monitored by incubating the cells with 0.3 μCi/well of ^{3}H-TdR overnight followed by harvesting and counting the incorporated radioactivity.

Staining of cultured breast cancer cells with anti-ECM1. The breast cancer cells were cultured in 8 well chamber slides overnight, fixed with 3.7% formalin for 5 minutes, stained with rabbit anti-ECM1b (1:400), followed by biotinylated goat anti-rabbit (1:250), peroxidase labeled streptavidin and the peroxidase substrate 3-amino-9-ethyl-carbazole and H_2O_2 which gives a dark red reaction product[27]. The cells were counter-stained with hematoxylin (blue) and preserved with CrystalMount (Biomeda Corp. Foster City, CA).

Western blotting for ECM1 in lysates of breast cancer cell lines: Cell lysates containing 30 μg of protein from different breast cancer cell lines were electrophoresed on a 10% SDS-polyacrylamide gel, transferred to a nitrocellulose membrane and incubated with rabbit anti-ECM1b (1:1000), peroxidase labeled anti-rabbit antibodies (1:4,000) followed by ECL.

Immunohistochemical staining for ECM1 in tissue specimens: Paraffin sections of human tissue containing normal, primary and secondary breast cancer were incubated with affinity purified anti-ECM1b, which only cross-reacted with ECM1a (1:400), followed by biotinylated goat anti-rabbit, peroxidase-labeled streptavidin and finally the substrate 3-amino-9-ethyl-carbazole and H_2O_2 (red). The sections were counter-stained with hematoxylin and preserved with CrystalMount.

Chick CAM assay for angiogenesis: This assay was performed according to the methods of Brooks *et al.* with some modifications[28]. The top air sac portions of 7-day-old chicken eggs were opened and the CAMs exposed. Two days later, filter disks (0.5 cm diameter) containing varying concentrations

of ECM1 and VEGF (15 μl containing 0, 0.5, 1, and 2 μg) were applied to the CAMs. Each group consisted of 10 eggs. Additional ECM1 and VEGF were applied to the filter discs for each of 3 days. On day 4, the CAMs and associated discs were cut out and immersed immediately in 3.7% formaldehyde. For computer analysis, the discs were divided into 4 quarters with fine wires. The blood vessels in each quarter of the CAM were digitally photographed and the results were analyzed by an *Optimas 5* program to calculate the vessel area and length in the viewing area. The total length and area of the vessels in the 4 quadrants of each disc were normalized to the total area measured and expressed as vessel length or area index. The means and the standard errors were calculated from all quadrants of all discs in each group and the statistical significance was examined by *student t test*.

RESULTS

Expression of ECM1 is closely associated with angiogenesis in the mouse embryo

In initial experiments, we examined the expression of Ecm1 (mouse abbreviation is Ecm1, human ECM1) mRNA in embryonic mice, using *in situ* hybridization with anti-sense RNA. As shown in Fig. 1 of a 12.5 day mouse embryo, a strong ECM1 signal was detected in almost all of the newly-formed blood vessels. The mRNA for ECM1 was particularly prominent in the endothelial cells lining the heart, aortic arch, pulmonary trunk, thoracic aorta and dorsal aorta (Figs. 1 A, C and E). In the brain, the signal formed a striated pattern, indicative of new blood vessels (Fig. 1 G). Additional studies indicated that this pattern of ECM1 expression occurred only during specific stages of embryonic development. In younger embryos, (embryonic day 7.5) a strong ECM1 signal was detected in the trophoblast, but not in blood islands, and in the angiogenic extra-embryonic tissue of the decidua where it formed a gradient with the highest concentration on the mesometrial side (data not shown). At later stages (embryonic day 15.5), the signal dramatically decreased in the central nervous system and completely disappeared from the walls of arteries and heart (data not shown). Thus, the expression of ECM1 in blood vessels occurs during a specific window of embryonic development in the mouse.

As shown in Figs. 1 G and H, the expression pattern of ECM1 in the central nervous system was very similar to that of the VEGF receptor flk-1, a marker of endothelial cells[7]. The most striking difference between flk-1 and ECM1 was in the timing of their expression. As previously reported, flk-1 mRNA persists throughout postnatal development[7]. In contrast, Ecm1 mRNA was dramatically down-regulated during later stage of gestation and coincided with the establishment of the blood-brain barrier on embryonic day 14.5[8]. These results suggested that ECM1 was closely associated early stages of angiogenesis and prompted us to investigate its role in this process.

ECM1 binds to glycosaminoglycans

One characteristic of VEGF and FGFs is that they can bind to heparin and other negatively-charged glycosaminoglycans[9-12]. To determine if ECM1 has similar properties, we examined its interaction with

heparin and hyaluronan (HA). When highly-purified preparations of recombinant ECM1a or ECM1b were added to ELISA plates with immobilized heparin or HA, these proteins bound in a dose-dependent manner and this binding was inhibited by soluble glycosaminoglycans (Fig. 2 A and B). Conversely, when HA was added to plates with immobilized ECM1a, it bound in a dose-dependent fashion (Fig. 2 C). Similarly, the binding of ECM1a to heparin-Sepharose 4B or HA-Sepharose 4B beads was inhibited by an excess of soluble heparin or HA (Fig. 2 D) while no staining was apparent in the negative controls (beads alone or soluble heparin and HA alone). These results indicate that both forms of ECM1 are capable of binding to heparin and HA, a property shared by other angiogenic factors.

ECM1 stimulates *in vitro* proliferation of cultured endothelial cells but not tumor cells

Next, we examined the ability of ECM1 to promote endothelial cell proliferation. Recombinant ECM1a was added to the culture media of three different sources of endothelial cells (HUVEC from human umbilical vein endothelial cells; BAEC from bovine aortic endothelial cells, and BREC from bovine retinal endothelial cells). In each case, ECM1a stimulated the proliferation of these endothelial cells with the optimal dose at 20 ng/ml (Fig. 3 A). Similar results were obtained with ECM1b except that the peak dose occurred at 50 ng/ml (data not shown). In contrast to endothelial cells, ECM1a did not stimulate the proliferation of breast tumor cell lines such as MDA-435 (Fig. 3 B) and MDA-468 cells (data not shown). Thus, ECM1 appears to specifically stimulate the proliferation of endothelial cells.

ECM1 enhances angiogenesis *in vivo*

To test whether ECM1 acts as an angiogenic factor *in vivo*, we examined its effect on the chick chorioallantoic membrane (CAM) assay. Recombinant ECM1a and ECM1b were adsorbed by small pieces of filter paper that were then placed on the CAM of chicken eggs. Two days later, the CAM associated with the filters were photographed. Figure 4 B through D shows that ECM1a stimulated angiogenesis in a dose-dependent fashion, and a similar effect was obtained with ECM1b (Fig. 4 E). The effects were comparable to that of VEGF which was used as positive control (Fig. 4 F). Image analysis of

these tissues revealed that both the vessel length and area indices (Figs. 4 G and H) were stimulated by the application of ECM1a and ECM1b. These results suggest that ECM1 promotes angiogenesis.

Expression of ECM1 protein in human breast cancer

In many cases, tumor cells have been shown to secrete angiogenic factors that are associated with malignant progression[13-16]. Furthermore, some tumor cells express proteins that are normally present only during embryonic development[17-19]. Consequently, we decided to determine if tumor cells also express ECM1 by Western blotting using antibodies specifically directed against ECM1. In initial experiments, we tested a panel of human breast cancer cell lines (Hs578T, MDA-468, MDA-435, Sk-Br-3, ZR571, T47D, and MCF-7) with anti-ECM1 and found that only the MDA435 cell line expressed high levels of ECM1 protein (Fig. 5). Based upon its size (68 kDa), we believe that it is ECM1a, since the purified recombinant ECM1a from CHO cells yielded a similar single band at 68 kDa (data not shown). Interestingly, in our hands, the MDA-435 cells were also the most malignant as judged by their growth in nude mice (unpublished observations). Subsequently, we have found that other cell lines also express ECM1, such as LCC15 that was derived from a bone metastasis of breast cancer[29]. The expression of ECM1 in malignant tumor cells suggests that it may play a role in tumor progression.

In cultured MDA-435 cells, ECM1 was seen focally in the cytoplasm, probably associated with organelles of the secretory pathway (Fig. 6 D). While MDA-435 cells produced ECM1, this protein did not stimulate the growth of these cells in tissue culture (Fig. 3 B), suggesting that any possible tumor-promoting function of ECM1 is not autocrine, but mainly due to its paracrine effects on angiogenesis.

To determine how widespread the expression of ECM1 was *in situ*, specimens of both primary and secondary tumors from human breast cancer patients were stained immunohistochemically. Figure 7 shows examples in which ECM1 was detected in primary breast cancer cells (Figs. 7 A and B) and secondary tumors formed in the lymph nodes (Fig. 7 C) and bone marrow (Fig. 7 D). In contrast, little or no staining was apparent in the normal breast ductal cells, stromal fibroblasts, and other inflammatory cells (Fig. 7 short arrows). Of the definitive breast cancer biopsies that we tested, 68% (21 out of 31)

were positive for ECM1. Of these, 12 out of 18 cases were metastatic tumors and 9 out of 13 cases were primary tumors. Thus, the expression of ECM1 is frequently associated with breast cancer cells.

DISCUSSION

In this study, we have presented several lines of evidence that ECM1 acts as a novel angiogenic factor. The most direct evidence came from the fact that ECM1 stimulated the proliferation of cultured endothelial cells, but not other tumor cell types that we tested such as MDA435 and MDA468. In this regard, ECM1 appears to be similar to VEGF in that its mitogenic activity is restricted to endothelial cells[14, 15]. However, its biological activity also extends to a number of other cell types like chondrocytes (Deckers *et al.*, submitted for publication). Additional evidence for ECM1's angiogenic properties came from experiments in which recombinant protein was applied to the CAMs of chicken embryos. As determined by computer-assisted image analysis, the ECM1 increased both the length and area of blood vessels in the CAM. Furthermore, the potency of ECM1 was comparable to that of VEGF, a well-known angiogenic factor. More indirect evidence that ECM1 is an angiogenic factor was suggested by its ability to bind glycosaminoglycans. This is probably due to an ionic interaction between the positively charged domains in ECM1 and the negative charges of the glycosaminoglycans. It is possible that binding of ECM1 to glycosaminoglycans in the extracellular matrix may modulate its biological activity, as is the case with FGFs and VEGF[20, 21]. Taken together, these results suggest that ECM1 plays a role in angiogenesis.

Our *in situ* hybridization studies have indicated that ECM1 mRNA is closely associated with blood vessels at different stages of mouse embryogenesis, particularly in mid-gestation. The signal is present in endothelial cells and its distribution is very similar to that of flk-1 (one of receptors for VEGF), identified as a marker for endothelium[7]. However, unlike flk-1, Ecm1 mRNA expression was down-regulated before birth. We suggest that Ecm1 is a novel marker for embryonic angiogenesis. This could also account for the fact that high levels of ECM1 are present in the placenta that contains numerous newly-formed blood vessels[3].

Another organ system in which ECM1 may be active is the skin. The mRNA of Ecm1 is associated with mouse epidermis, but not the underlying dermis (Smits *et al.*, submitted for publication). It is tempting to speculate that epidermal keratinocytes secrete ECM1 into the adjacent dermis and stimulate the formation of blood vessels. Functionally, this area requires a high degree of vascularization so that the avascular epidermis can receive oxygen and other nutrients from underlying dermis for their proliferation. We speculate that the ability of ECM1 to interact with glycosaminoglycans may be important to limit its diffusion *in vivo* such that its highest concentration is at the boundary between the dermis and epidermis such that most blood vessels form in this region.

ECM1 may also play a role in tumor angiogenesis, which is a prerequisite for rapid tumor growth and metastasis[13-15]. In many cases, tumor cells facilitate their own progression by directly producing angiogenic factors or by inducing other cells to synthesize them[13-15, 22]. It is possible that ECM1 represents a new factor among those produced by tumor cells (such as MDA 435 and LCC-15) to promote their progression. In our hands, the MDA-435 line was also the most aggressive with respect to growth in nude mice (unpublished observations). More importantly, when both primary and secondary breast cancer tissues were tested for ECM1, a relatively high proportion of the tumor cells were positive. In contrast, we found little or no positive staining in normal breast ductal epithelial cells, fibroblasts, leukocytes and other stromal cells. Thus, it appears that at least a proportion of tumor cells produce ECM1 which could stimulate their vascularization and promote their progression. If this turns out to be the case, then this protein could be used as a target for anti-tumor therapy.

Acknowledgments

We thank Drs. Stephen Byers and Robert Dickson for the critical review of the manuscript and Dr. Susette C. Mueller for the guiding of using the computer imaging analysis. This work was supported in part by NCI/NIH (R29 CA71545), U. S. Army Med. Res. & Mat. Command (DAMD 17-98-1-8099) and Susan G. Komen Breast Cancer Foundation to L.Z. and U. S. Army Med. Res. & Mat. Command (DAMD 17-94-J-4284 and PC970502) as well as Susan G. Komen Breast Cancer Foundation to C.B.U. J.M. and D. H. were supported by G.0085.98 from the Fund of Scientific Research-Flandres.

REFERENCES

1. Mathieu E., Meheus, L., Raymackers, J. and Merregaert, J. (1994) *J.Bone Miner Res.* **9**, 903-913
2. Smits P, Ni J, Feng P, Wauters J, Van Hul W, Boutaibi ME, Dillon PJ, Merregaert J. (1997) *Genomics* **45** (3), 487-95
3. Johnson MR, Wilkin DJ, Vos HL, Ortiz de Luna RI, Dehejia AM, Polymeropoulos MH, Francomano, CA. (1997) *Matrix Biol* **16** (5), 289-92
4. Bhalerao J, Tylzanowski P, Filie JD, Kozak CA, Merregaert, J. (1995) *J Biol Chem.* **270** (27), 16385-16394
5. Yang , F., Brune, J., Naylor, S., Cupples, R., Naberhaus, K., and Bowman, B. (1985) *Proc.Nalt.Acad. Sci. USA* **82**, 7994-1998
6. Kragh-Hansen,U. (1990) *Danish Med. Bull.* **37,** 57-84
7. Millauer B, Wizigmann-Voos S, Schnurch H, Martinez R, Moller NP, Risau W, Ullrich, A. (1993) *Cell* **72**(6), 835-846
8. Hoffmann A, Bachner D, Betat N, Lauber J, Gross, G. (1996) *Dev Dyn* **207**(3):332-343
9. Jackson, R. L., Busch, S. J., and Cardin, A. D. (1991) *Physiol. Rev.* **71**, 481-539
10. Weinstat-Saslow, D. and Steeg, P. S. (1994) *FASEB J.* **8**, 401-407
11. Miller, M. D. and Krangel, M.S. (1992) *Crit. Rev. Immunol* **12**, 17-46
12. Zhang, L., Kharbanda, S., Chen, D., Bullocks, J., Miller, DL., Ding, IY., Hanfelt, J., McLeskey, W., Kern, FG. (1997) *Oncogene* **15**(17), 2093-2108
13. Folkman, J. and Shin, Y. (1992) *J. Biol. Chem.* **267**, 10931-10934
14. Plate, K. H., Breier, G., Weich, H. A., and Risau, W. (1992) *Nature (Lond.)* **359**, 845-847
15. Kim, K. J., Li. B., Winer, J., Armanini, M., and Gillet, N. (1993) *Nature (Lond.)* **362,** 841-844

16. Nabal, E. G., Yang, Z., Plants, G., Forough, R., Zhang, S., Haudenschild, C.C. Macaig, T. and Nabel, G. J. (1993) *Nature (Lond.)* **362,** 844-846

17. Kew, M.(1974) *Gut* **15**(10), 814-821

18. Jacob, F. (1983) *Ciba Found Symp* **96**, 4-27

19. Yachnin, S. (1978) *Ann Clin Lab Sci* **8**(2), 84-90

20. Breier, G., Clauss, M., Risau, W. (1995) *Dev Dyn* **204** (3), 228-239

21. Kan, Mikio., Wang, Fen., Xu, J., Crabb, J. W., Hou, J., McKeehan, W. L. (1993) *Science* **259,** 1918-1921

22. Rosen, E. M., Knesel, J. and Goldberg, I.D. (1991) *Cell Growth Diff.* **2,** 603-607

23. Dewulf, N., Verschueren, K., Lonnoy, O., Morén, A., Grimsby, S., Vande Spiegle, K., Miyazono, K., Huylebroeck, D. and Ten Dijke, P. (1995) *Endocrinology* **136**, 2652-2663

24. Ni, J., Abrahamson. M., Zhang, M., Fernandez, M., Grubb, A., Su, J., Yu, G-L., Li, Y-L., Parmelee, D., Xing, L., Coleman, T., Lima, S., Thotakura, R., Nguyen, N., Hesselberg, M., Gentz, R. (1997) *J Biol Chem* **272**, 10853-10858

25. Ni, J., Fernandez, MA., Danielsson, L., Chillakuru, RA., Zhang, J., Grubb, A., Su, J., Gentz, R., Abrahamson, M. (1998) *J Biol Chem* **273,** 24797-24804

26. Tengblad, A. (1979) *Biochimica Biophysica Acta.* **578**(2), 281-289

27. Green, S. J., Tarone, G. and Underhill, C. B. (1988) *J. Cell Sci.* **89,** 145-156.

28. Brooks, P. C., Silletti, S., von Schalscha, T. L., Friedlander, M., Cheresh, D. A. (1998) *Cell* **92**(3), 391-400

29. Sung, V., Gilles, C., Murray, A., Clarkem R., Aaron, A. D., Azumi, N., Thompson, E. W. (1998) Exp Cell Res **241**(2), 273-84

FIGURE LEGENDS

Fig. 1. *In situ* hybridization of ECM1 and flk-1 mRNA in mid-gestation mouse embryos. The mRNA transcript of Ecm1 in a 12.5 day mouse embryo was detected with a probe consisting of a ^{35}S-dATP-labeled, 512 bp anti-sense sequence of the 5' region of mouse Ecm1. **(A and B)** Dark and light field views of ECM1 message in a sagittal section through the embryo at low magnification . The following structures have been labeled: N, neural tube; H, heart; D, dorsal aorta; A, aortic arch; and P, pulmonary trunk. **(C and D)** Dark and light field views of ECM1 message in a sagittal section of the neural tube at higher magnification. The label is associated with the newly forming blood vessels. The following structures have been labelled: C, central canal of spinal cord; B, blood vessel; N, neural tube. **(E and F)** Dark and light field views of the of: A, the aortic arch; and P, the pulmonary trunk P. Label is associated with the cells lining both of these blood vessels. **(G and H)** Dark field views of the developing brain showing the distribution of ECM1 and flk-1 message respectively. The pattern is very similar for both of these messages, and flk-1 is a marker for endothelial cells.

Fig 2. Binding of human ECM1 to glycosaminoglycans. **(A and B)** Interaction between ECM1 and immobilized glycosaminoglycans. The wells of ELISA plates were coated with either heparin or HA, and then varying concentrations of ECM1a or ECM1b with or without preincubation with 30 μg of HA or 20 U of heparin were added to the wells. The amount of protein bound to the plate was then determined by an ELISA with affinity purified rabbit anti-ECM1. **(C)** Binding of HA to immobilized ECM1. A plate was coated with recombinant ECM1a and then incubated with varying concentrations of HA. The bound HA was as detected by an ELISA using affinity purified biotinylated HA binding protein. **(D)** The interaction of ECM1 with glycosaminoglycans analyzed by immunoprecipitation and Western blotting. Soluble ECM1a (1 or 5 μg) with or without preincubation with soluble heparin or HA was mixed with heparin-Sepharose or HA-Sepharose. After washing, the bound ECM1 was disassociated with Laemmli

sample buffer, electrophoresed on a 10% SDS-polyacrylamide gel, and transferred to a nitrocellulose membrane. The ECM1 was detected by Western blotting using affinity purified anti-ECM1 antibody and a chemoluminescent substrate for peroxidase. Similar results were obtained from three repeated experiments.

Fig 3. Effect of ECM1 on cell proliferation. Varying amounts of ECM1a were added to the medium of cultured cells and the effects on proliferation were determined by the incorporation of ^{3}H-TdR **(A)** ECM1a stimulated the proliferation of HUVEC with a optimal effect at 20 ng/ml ($P<0.01$). Similar results were also obtained with the ABAE and BREC cell lines. **(B)** The addition of ECM1 to the medium of MDA-435 had little or no effect on the proliferation of these cells ($P>0.05$ in all groups). Similar results were obtained with MDA-468 cells. Four individual experiments yielded similar results.

Fig. 4. *In vivo* stimulation of angiogenesis by ECM1 on the chicken CAM. The filter discs containing varying amounts of ECM-1 were placed on the CAMs of 9 day-old eggs and harvested on day 11. Photographs representative of each condition are shown. **(A)** PBS control; **(B)**: 0.5 μg of ECM1a; **(C)** 1 μg of ECM1a; **(D)** 2 μg of ECM1a; **(E)** 2 μg of ECM1b; and **(F)**: 2μg of VEGF as a positive control. **(G and H)** For computerized image analysis of the angiogenesis indices, each filter disc was divided into 4 quarters by fine wires and all of the vessels in each quarter were digitally photographed. The ratio of length and area of vessels relative to the total area in each sample was determined with an *Optimas 5* program and expressed as an index. The means and standard errors of the ratios from each group (with 40 individual samples) were calculated and analyzed statistically (* stands for $P<0.05$).

Fig. 5. Detection of ECM1 in cell lysates of breast cancer cells by Western blotting. Lysates from different breast cancer cell lines were electrophoresed on a 10% SDS-polyacrylamide gel, transferred to a nitrocellulose membrane and incubated sequentially with rabbit anti-ECM1 antibodies, peroxidase

coupled anti-rabbit antibodies and finally a chemoluminescent substrate (ECL). Similar results were obtained in three separate experiments.

Fig. 6. Expression of ECM1 in cultured breast cancer cells. MCF-7, MDA-436, MDA-468 and MDA-435 cells were cultured in an 8 well-chamber slide and then fixed, stained with antibodies to ECM1 and detected using immuno-peroxidase that gave rise to a dark red reaction product. **(A, B and C)** Representative sections show that MCF-7, MDA-436 and MDA-468 cells are negative for staining with anti-ECM1; **(D)** MDA-435 cells showed strongly positive staining in the cytoplasm (Bar = 5 μm).

Fig. 7. Expression of ECM1 in sections of primary and secondary breast cancers. Paraffin sections of human breast cancer tissues were stained for ECM1 using specific antibodies with a peroxidase coupled system (red reaction product) and then counter-stained with hematoxylin (blue). **(A and B)** While the normal ductal epithelial and stromal cells (small arrow in A) showed little or no staining, the primary cancer cells (large arrows) stain positive (red). **(C)** Metastatic breast cancer cells in the lymph node also showed positive staining (large arrow indicates tumor, small arrow indicates normal lymph node tissue). **(D)** Metastatic breast cancer cells in the bone show positive staining (large arrow indicates breast cancer cells; short arrows indicate the normal cells in the tissues). (Bar = 10 μm).

Figure 1a

Han,et al

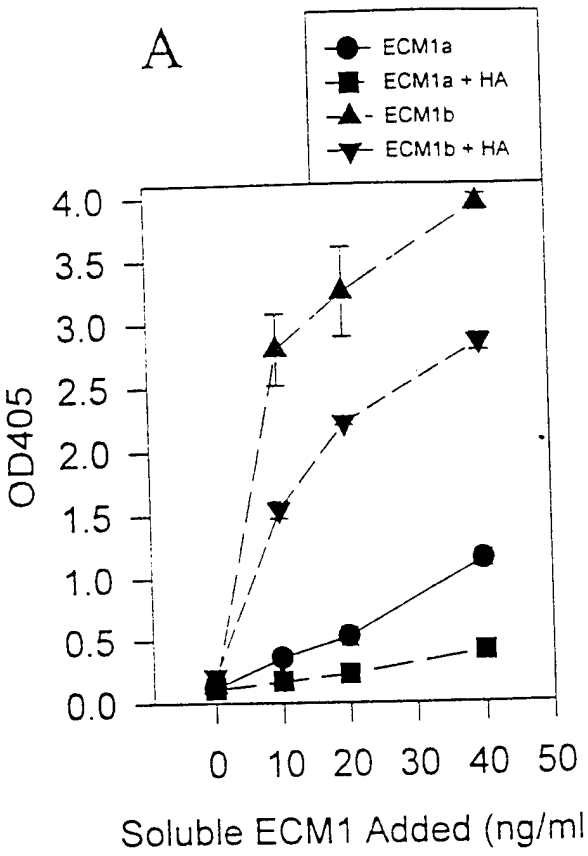

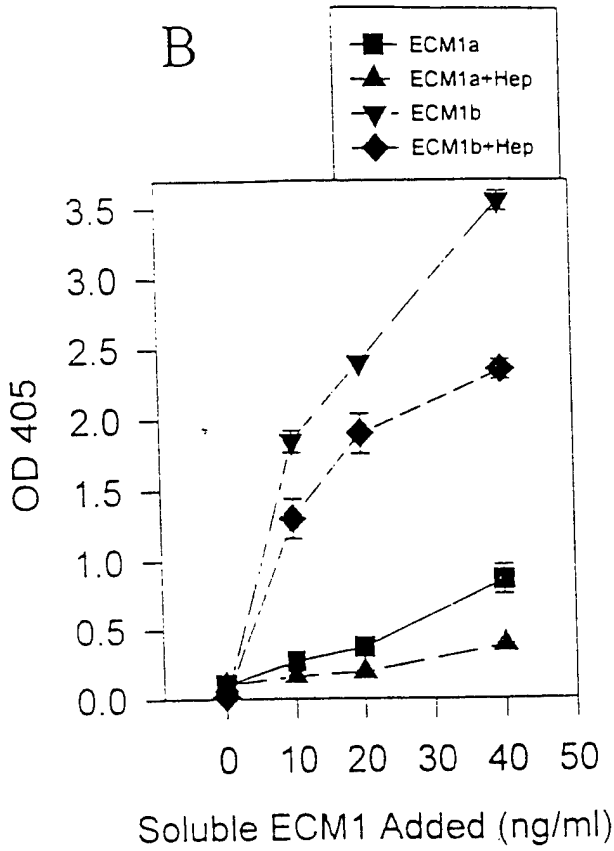

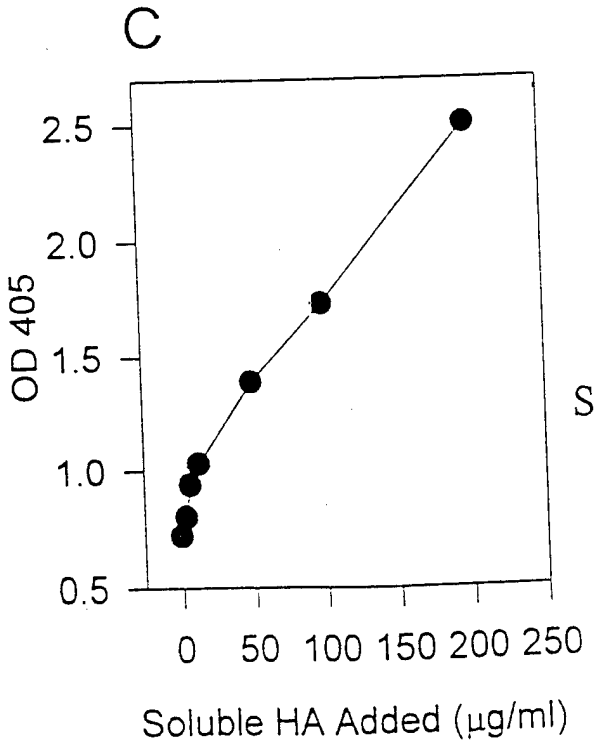

D

ECM1a	5 µg	5 µg	1 µg	1 µg
Heparin-4B	+	+	-	-
HA-4B	-	-	+	+
Soluble heparin	+	-	-	-
Soluble HA	-	-	+	-

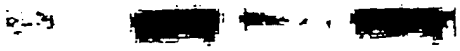

Figure2, Han, et al

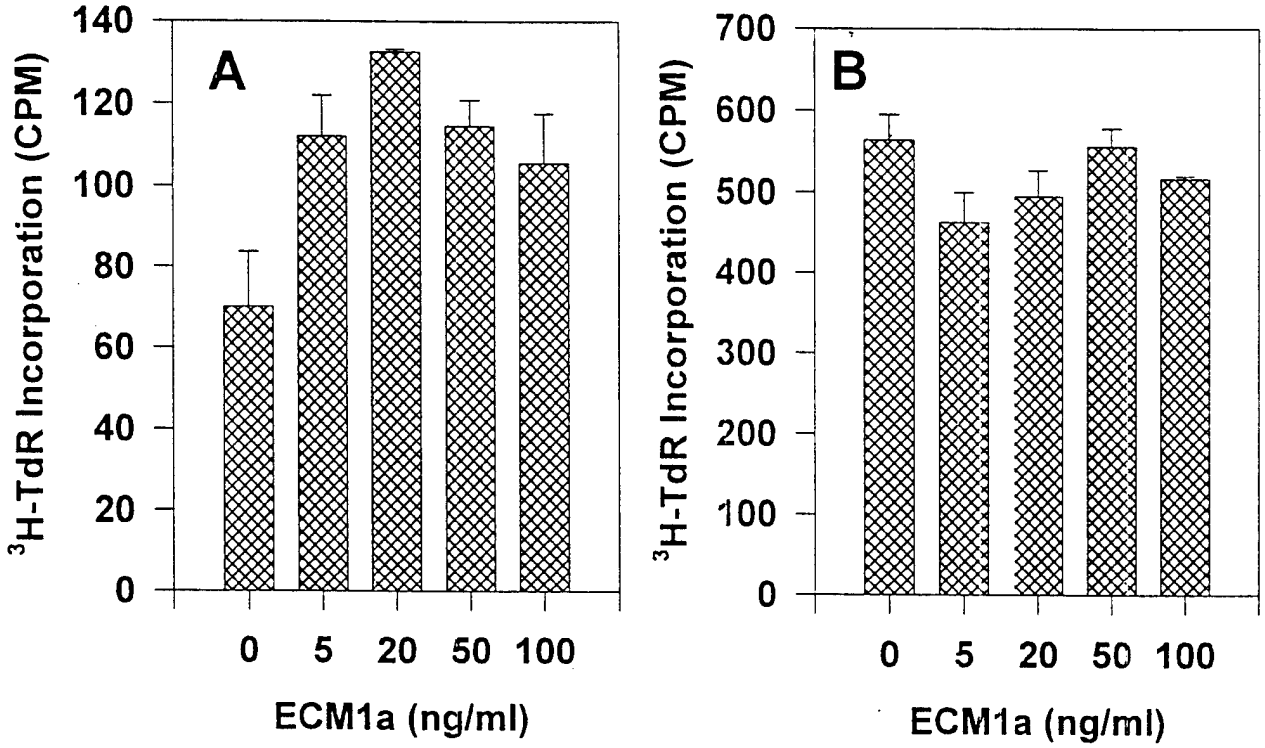

Figure 3

Han, et al

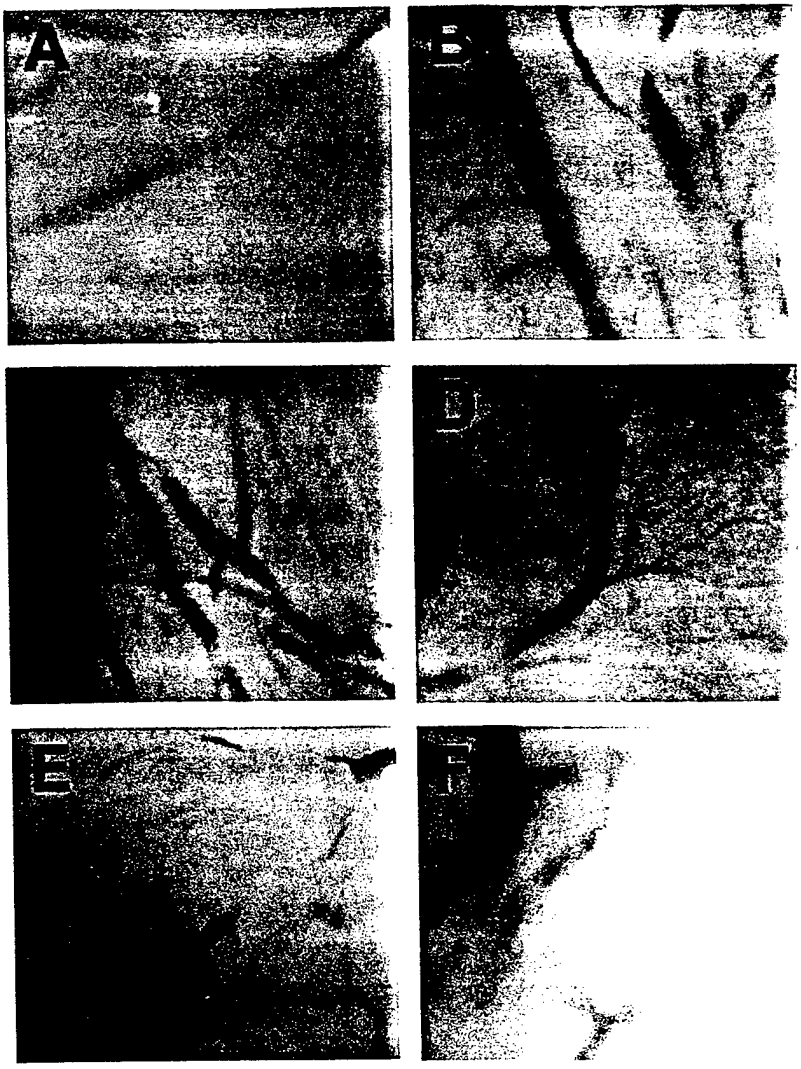

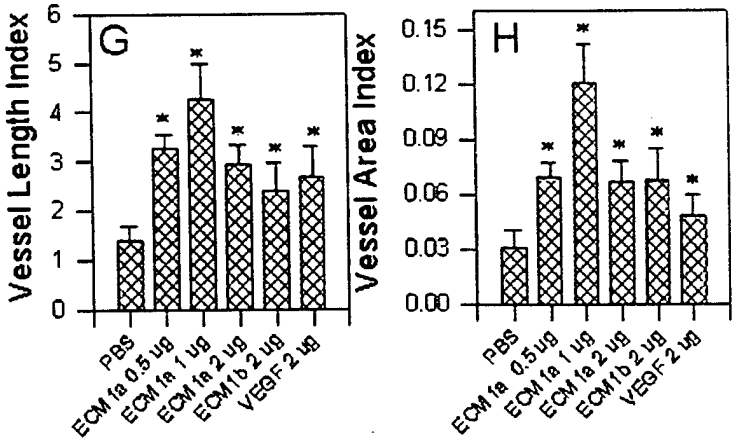

Figure 4, Han, et al

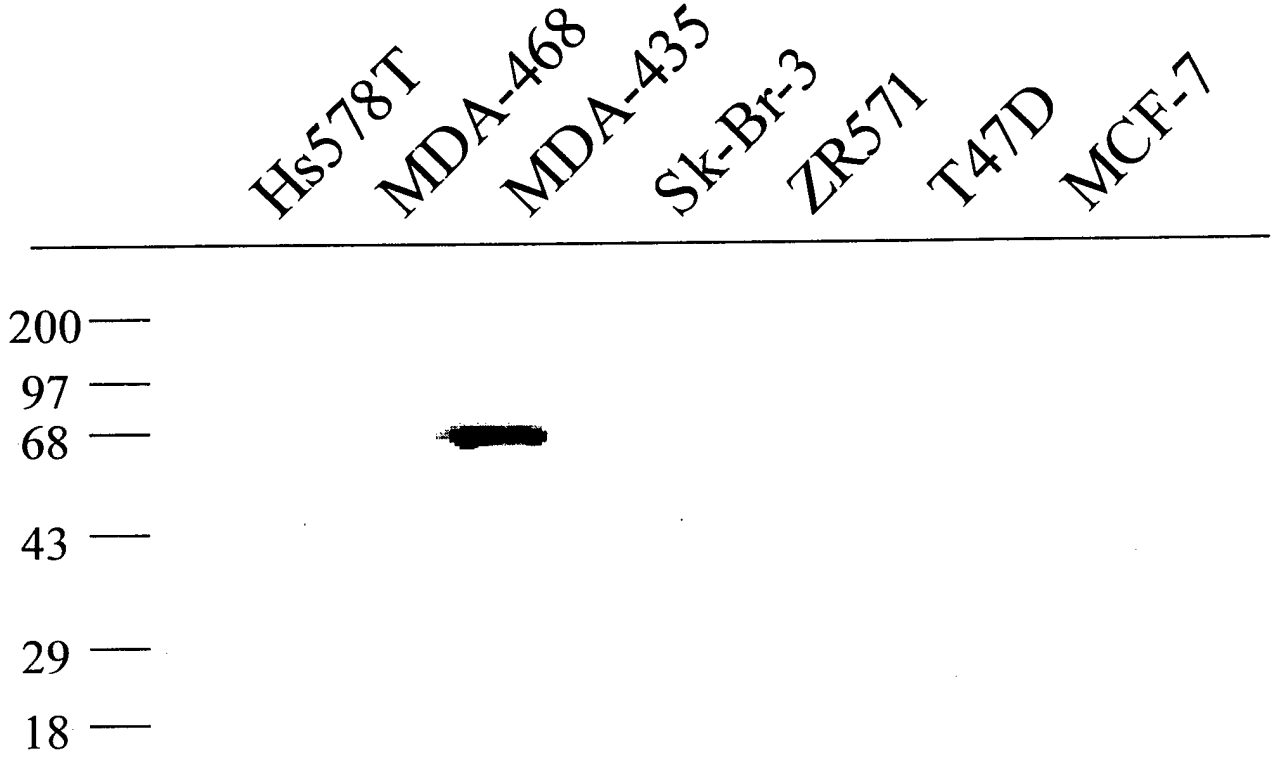

Figure 5, Han, et al

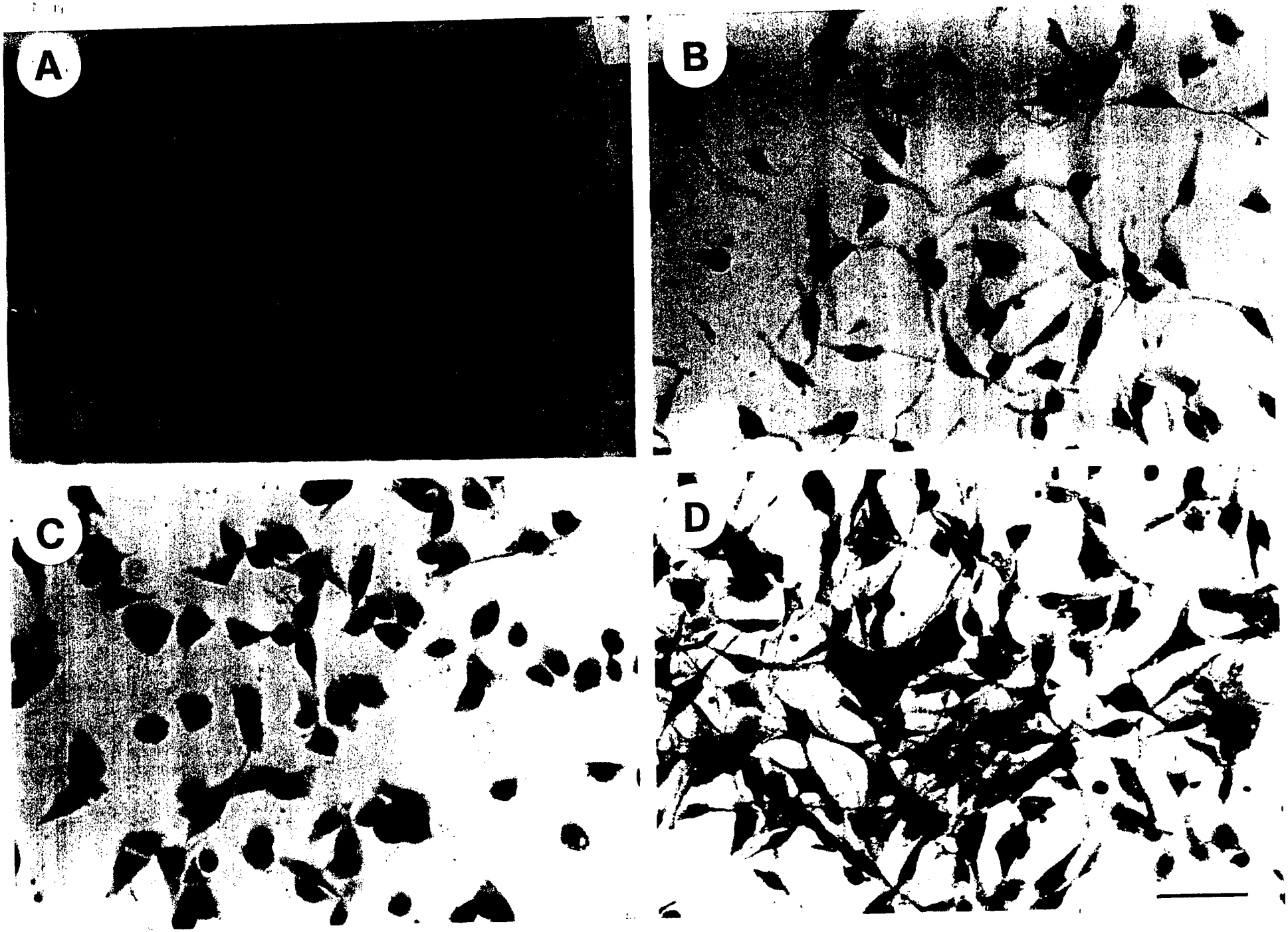

Figure 6, Han, et al

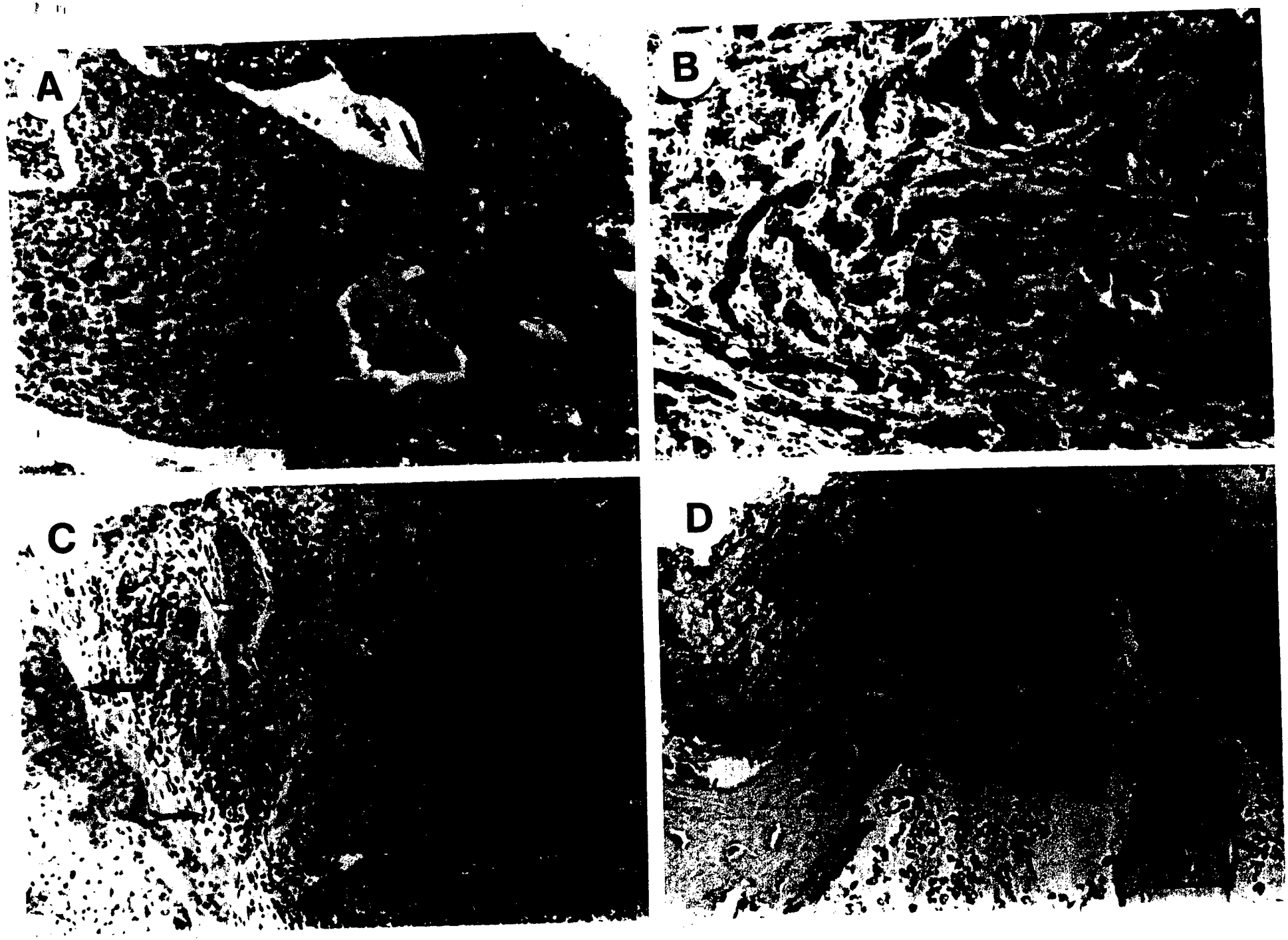

Figure 7, Han, et al

Job: Tuan 3 (576-X)
Chapter: 40/Underhill
Pub Date: 11/99

Operator: KB
Date: 7/27/99
Revision: 1st gal/rough paging

Please note: On my FAX many of the e's appear as ę's. This is probably due to the poor quality of the FAX, but just to be on the safe side, I have indicated these words in the margins

Analysis of Hyaluronan Using Biotinylated Hyaluronan-Binding Proteins

<Au: Pls. proofread carefully.

Charles B. Underhill and Lurong Zhang

1. Introduction

In this chapter, we describe the preparation and use of b-PG, a biotinylated complex that specifically binds hyaluronan *(1,2)*. The b-PG is derived from cartilage and consists of a trypsin fragment of the proteoglycan core protein and one of the link proteins. Because of its ability to bind to hyaluronan with high affinity and specificity, the b-PG agent has proved to be useful in the histochemical localization of hyaluronan and its quantitative analysis by an enzyme linked assay *(1,2)*.

The b-PG reagent described here has evolved from several earlier versions. The first use of fluorescently tagged cartilage proteins for histochemistry of hyaluronan was described by Knudson and Toole *(3)*. Shortly after, Ripellino et al. described the use of a biotinylated reagent that was isolated from cartilage by ultracentrifugation *(4)*. The present protocol consists of a modification of one originally described by the late Dr. A. Tengblad that involves the use of affinity chromatography *(5)*. It should be acknowledged that the procedure describe here draws heavily from the excellent work of Dr. Tengblad.

while → ~~Because~~ b-PG is a very useful reagent, its preparation is a major undertaking. The synthesis of HA-Sepharose and the purification of b-PG is both expensive and time consuming. Once the HA-Sepharose has been prepared, the isolation of b-PG takes about 2 wk. In general, we prepare several batches of the b-PG at one time, until we have exhausted our supply of cartilage extract. On the positive side, the HA-Sepharose can be reused many times, and the preparations of b-PG can be stored under the appropriate conditions for a number of years without loss of activity.

<Au: Pls. provide lab and location.

In the following sections we will describe:

1. The preparation of HA-Sepharose;
2. The isolation of b-PG;
3. The use of b-PG in histochemistry; and
4. The quantitative analysis of hyaluronan using b-PG in an enzyme linked assay.

Georgetown Medical Center
Lombardi Cancer Center
Research Bld, EG-19A
Washington DC 2007

From: *Methods in Molecular Biology, Vol. 137: Developmental Biology Protocols, Vol. III*
Edited by: R. S. Tuan and C. W. Lo © Humana Press Inc., Totowa, NJ

Job: Tuan 3 (576-X)
Chapter: 40/Underhill
Pub Date: 11/99

Operator: KB
Date: 7/27/99
Revision: 1st gal/rough paging

2. Materials

2.1. Preparation of HA-Sepharose

1. The NH_2-derivatized matrix, EAH Sepharose 4B is purchased from Pharmacia Biotech (Uppsala, Sweden). In general, we use 100 mL (two batches) of the matrix for each preparation. Alternatively, the derivatized matrix can be prepared according to the methods described by Cambiaso et al. *(6)*.
2. Highly purified hyaluronan of approx 7×10^5 molecular weight is obtained from Lifecore Biomedical (Chaska, MN).
3. Testicular hyaluronidase (type VI-S), 1-ethyl-3-(3-dimethylamino-propyl)carbodiimide and the other incidental reagents are obtained from Sigma Chemical Co. (St. Louis, MO).

2.2. Isolation of b-PG

1. Bovine nasal cartilage is purchased from Pel-Freez (Rogers, AR).
2. For processing of the cartilage, we use a Surform pocket plane (Stanley Tools) that is available in most hardware stores and cheese cloth that can be obtained at most grocery stores. In addition, large size dialysis tubing (3.3-cm Spectrapor membrane tubing) was used. In place of a Surform plane, a meat grinder may also be used.
3. Trypsin (type III) and soybean trypsin inhibitor (Type I-S) are both obtained from Sigma.
4. The biotinylating reagent Sulfo-NHS-LC-Biotin (EZ-Link) is obtained from Pierce (Rockford, IL).
5. Because the procedure requires large amounts of 4 *M* guanidine HCl, 0.5 *M* Na acetate pH 5.8, it is worthwhile to purify crude preparations of this reagent. To do this, 1528 g of practical grade guanidine HCl (Sigma) and 272 g of Na acetate-3 H_2O is dissolved in water, the pH is adjusted to 5.8 and the volume to 4 L. A tablespoon full of decolorizing carbon (Norit, Baker, NJ) is added to the solution which is stirred for 1 h. The solution is then passed through a Whatman filter on Buchner funnel and stored for use.

2.3. Histochemistry for Hyaluronan

1. The normal histochemical reagents consist of a clearing agent (Americlear), ethyl alcohol, and 30% H_2O_2.
2. A 10X stock solution of calcium–magnesium-free phosphate-buffered saline (PBS-A) is prepared from the following: 80 g NaCl, 2.0 g KH_2PO_4, 2.0 g KCl, and 11.5 g Na_2HPO_4 dissolved in 1 L of water. After diluting 1 to 10, the pH should be 7.3.
3. The reagent buffer consists of 90% PBS-A, 10% calf serum which should be passed through a 0.45 µ filter prior to use. This may be frozen in 10-mL aliquots.
4. Streptavidin-horse radish peroxidase can be purchased from Kirkegaard and Perry (Gaithersburg, MD).
5. The 3-amino-9-ethylcarbazole, dimethyl formamide (or dimethyl sulfoxide) and Mayer's hematoxylin solution are purchased from Sigma.
6. Crystal/mount to preserve the chromogens is purchased from Biomeda (Foster City, CA).

2.4. Enzyme Linked Assay for Hyaluronan

1. Hyaluronan was purchased from Lifecore Biomedical.
2. Bovine serum albumin, 2,2'azinobis (3-ethylbenzthiazoline sulfonic acid), 1-ethyl-3-(3-dimethylamino-propyl)carbodiimide and NaN_3 are purchased from Sigma.

Job: Tuan 3 (576-X)
Chapter: 40/Underhill
Pub Date: 11/99

Operator: KB
Date: 7/27/99
Revision: 1st gal/rough paging

3. Methods

3.1. Preparation of HA-Sepharose

The b-PG is isolated by affinity chromatography on a matrix of hyaluronan coupled to Sepharose (HA-Sepharose). The preparation of the HA-Sepharose involves two steps. In the first step, hyaluronan is converted to an appropriate size so it can penetrate the gel, and in the second step it is coupled to an NH_2-derivatized gel using a carbodiimide cross-linking agent. ~~Because~~ while the preparation of this gel is expensive, it can be reused many times.

1. To convert hyaluronan to the appropriate size, 1 g of the hyaluronan is dissolved in 500 mL of 0.15 *M* NaCl, 0.15 *M* Na acetate pH 5.0 and then incubated with 4000 U of testicular hyaluronidase (type VI-S, Sigma) for 3 h at room temperature. The digestion is stopped by placing the sample in a boiling water bath for 20 min and then the sample is centrifuged (10,000*g*, 15 min) to remove any precipitate. Four volumes of ethyl alcohol are added to the solution, which is cooled to –20°C for 1 h and then centrifuged (10,000*g*, 15 min) and the pellet of digested hyaluronan is collected. The precipitate is washed once in 75% alcohol to remove the acetate buffer.
2. For the coupling reaction, the digested hyaluronan (approx 1 g) is redissolved in a small volume of distilled water, mixed with 100 mL of the EAH Sepharose 4B and brought to a final volume of 250 mL. The suspension is placed on a shaking table (to avoid shearing the beads with a magnetic stirrer), the pH is adjusted to 4.7 and 2 g of the coupling agent 1-ethyl-3-(3-dimethylamino-propyl) carbodiimide is added to the mixture. Thereafter, the pH is continuously adjusted to 4.7 until the reaction has been completed (approx 3 h).
3. The mixture is allowed to sit over night, and then 10 mL of acetic acid is added to the suspension for a period of 6 h to block residual coupling agent. The gel is then transferred to a Buchner funnel and washed sequentially with 1 L each of: (a) 1 *M* NaCl, (b) 0.05 *M* fomic acid, and (c) distilled water. The preparation is finally washed with 0.5 *M* Na acetate pH 5.7 plus a small amount of Na azide and is stored in this buffer at 4°C (*see* **Note 1**). The gel is stable for years.

<Au: fomic OK? formic? yes formic

3.2. Isolation of b-PG

The preparation of b-PG involves a number of steps. First, the extract is treated with trypsin to reduce its size. Second, the biotin-coupling reaction is carried out on the crude preparation so that endogenous hyaluronan protects the binding site. And finally, affinity chromatography is carried out taking advantage of the fact that the binding of aggrecan to hyaluronan is reversed by 4 *M* guanidine HCl.

1. The bovine nasal cartilage is thawed out and stripped of associated membranes with a pair of pliers, and then shredded with a Surform pocket plane. This step may take 1 d.
2. The shredded cartilage is weighed and mixed with 10 mL of 4 *M* guanidine HCl, 0.5 *M* Na acetate pH 5.8 for each gram of cartilage. The mixture is placed in a large beaker and placed on a shaking table at 4°C overnight (the solution is generally too thick to use a stirring bar).
3. To remove the solid material, pour the extract through several layers of prewashed cheese cloth. The fluid is then centrifuged (10,000g, 45 min, 4°C) and the supernatant is passed through a filter paper (Whatman no. 1, Whatman, Clifton, NJ) on a Buchner funnel.
4. The extract is then placed in large dialysis tubes (3.3 cm) and dialyzed against running tap water (leave plenty of room for the swelling of the dialysis bag because of osmosis).

plane = Note: make sure that this is plane not plane

Job: Tuan 3 (576-X)
Chapter: 40/Underhill
Pub Date: 11/99

Operator: KB
Date: 7/27/99
Revision: 1st gal/rough paging

Dialyze first against running tap water overnight and then against several changes of distilled water (it is necessary to remove the last traces of guanidine HCl that interfere with the biotin reaction).

5. The dialyzed extract is then lyophilized for long-term storage. For this, the extract is poured into ice cube trays, frozen, and then placed in a lyophilization bottle. This step may take several days (*see* **Note 2**).
6. Approximately 3 g of the lyophilized extract is mixed with 100 mL of 0.1 *M* HEPES, 0.1 *M* Na acetate pH 7.3, and is stirred overnight at 4°C to dissolve. The resulting mixture will be opaque and lumpy. In some cases, it may be desirable to further dialyze this sample against the above buffer to make sure that all of the guanidine has been removed.
7. Add 1.6 mg of purified trypsin to the mixture and then incubate at 37°C with occasional stirring. As the digestion progresses, the extract becomes less viscous. After 2 h, the digestion is stopped by adding 2 mg of soybean trypsin inhibitor and the pH is adjusted to 8.0.
8. Assay the protein content of the extract using a coomassie blue staining reagent (it should be between 5–10 mg/mL). Using the total amount of protein as a basis, add 1/10 the weight of sulfo-NHS-LC biotin to the sample. Allow the coupling reaction to proceed for 1–2 h at room temperature.
9. Dialyze the extract against three changes of 500 mL each of 4 *M* guanidine HCl, 0.5 *M* Na acetate, pH 5.8. The guanidine solutions can be reused several times for the first two changes, however, the final concentration of the extract should be close to 4 *M* guanidine HCl, 0.5 *M* Na acetate, pH 5.8.
10. Using a Buchner funnel, wash 100 mL of the HA-Sepharose with 4 *M* guanidine HCl, 0.5 *M* Na acetate, pH 5.8. and then transfer this gel to a beaker containing the extract. The mixture is poured into a large dialysis bag (leaving room for expansion) and placed in a beaker with nine volumes of distilled water. For the first 4 h, it is important to resuspend the beads that have settled out by inverting the bag upside down every 30 min. The beaker is then shaken overnight on a rotary table in the cold room.
11. Degas the mixture in a vacuum and pour into a column of the appropriate size. The gel is then washed with 200 mL of 1 *M* NaCl followed by a 400-mL linear gradient of from 1 to 3 *M* NaCl. At this point, the column is connected to a fraction collector (2.5 mL fractions) and the specifically bound proteins are eluted with 4 *M* guanidine HCl, 0.5 *M* Na acetate, pH 5.8. Each fraction is monitored for protein and those containing most of the protein are pooled and dialyzed against 0.15 *M* NaCl (*see* **Note 3**).
12. The concentration is adjusted to 200 µg/mL and then mixed with an equal volume of glycerol (100 µg/mL final concentration). Between 1 and 3 mg of the b-PG is generally obtained. This can be stored at –20°C, and is stable for a number of years (*see* **Note 4**).

3.3. Histochemistry of Hyaluronan with b-PG

The b-PG reagent is excellent for the histochemical localization of hyaluronan in tissue sections.

1. ~~Because~~ fixation in formaldehyde by itself results in adequate preservation, Lin et al. has found that acidformalin in 70% alcohol provides superior retention of hyaluronan (*7*). The use of cetylpyridinium chloride to help retain the hyaluronan is not advised.
2. The fixed tissue can then be processed and sectioned by a variety of techniques. These include direct cryostat sectioning, as well as paraffin and polyester wax embedding (*8*). Because hyaluronan has a very stable structure, preservation of its structural integrity is generally not a problem.

Job: Tuan 3 (576-X)
Chapter: 40/Underhill
Pub Date: 11/99

Operator: KB
Date: 7/27/99
Revision: 1st gal/rough paging

3. The sections are rehydrated, by two 5 min incubations in the following solutions. Clearing agent (Americlear); 100% ethyl alcohol; 95% alcohol, 75% alcohol, and then water. The sections are then incubated for 5 min in 10% H_2O_2 to inactivate endogenous peroxidases. The sections are then rinsed in two washes of water and finally in PBS-A.
4. The slides are placed on a moist sponge in a covered baking pan and overlaid with a solution of 8–10 µg/mL of b-PG dissolved in 10% calf serum, 90% PBS-A (make sure the sections do not dry out). After 1 h the slides are washed for 5 min in PBS-A.
5. The sections are incubated for 15 min with a 1–500 dilution of streptavidin coupled to horse radish peroxidase in 10% calf serum, 90% PBS-A. Following the incubation, the slides are washed for 5 min in PBS-A.
6. The sections are then incubated with substrate for horse radish peroxidase. We use 3-amino-9-ethylcarbazole that is particularly sensitive and gives rise to an intense red precipitate (*9*). This should be prepared immediately before use in the following manner:
   a. Dissolve 2 mg of 3-amino-9-ethylcarbazole in 0.5 mL of dimethyl formamide (or dimethyl sulfoxide).
   b. Mix with 9.5 mL of 0.05 *M* Na acetate, pH 5.0.
   c. Pass solution through a 0.45-µ filter. The solution should be clear at this point.
   d. Add 10 µL of 30% H_2O_2 (1 µL per mL).
   e. Apply substrate to the slides. The reaction product has an intense red color. The incubation time can vary from less than 5 min to more than 30 min depending upon the section. Monitor the progress of the reaction by observing the slide under low magnification.
   f. Stop the reaction by washing section in PBS-A (or distilled water for hematoxylin staining).
7. If counter staining is desired, then the section can be dipped in Mayer's hematoxylin for 4 min, and then washed sequentially in distilled water, PBS-A and finally distilled water.
8. For permanent preservation of the stain, the sections can be coated with Crystal/mount before attaching a cover slip.
9. To control for nonspecific staining, two different procedure may be used. First, the b-PG may be mixed with 0.1 mg/mL hyaluronan prior to application to the section. Alternatively, the sections may be pretreated with hyaluronidase. In our hands, the nonspecific staining is minimal (*see* **Note 5**).

3.4. An Enzyme-Linked Assay for Hyaluronan

This assay is based upon the ability of a sample of hyaluronan to bind to b-PG in solution and prevent it from binding to hyaluronan that is attached to a plastic substrate (*2*). In our hands, the assay is sensitive to concentrations of hyaluronan between 50 ng/mL and 1 µg/mL.

1. The first step of this protocol is to coat plates with hyaluronan. It is important to note that pure hyaluronan by itself does not attach to plastic surfaces or nitrocellulose (however, crude preparations of hyaluronan, which are often associated with protein, will stick via the protein). Our approach is to couple hyaluronan to bovine serum albumin (HA-BSA) that adheres tightly to the plastic. For this, 100 mg of hyaluronan is dissolved in 500 mL of 0.2 *M* NaCl and the pH is adjusted to 4.7. To this is added 100 mg of bovine serum albumin followed by 20 mg of 1-ethyl-3(3-dimethylaminopropyl) carbodiimide. The pH is maintained at 4.7 for 1 h and then the solution is dialyzed extensively against PBS-A. The HA-BSA was aliquoted into 96 well plates (100 µL/well) and incubated for 30 min. The wells of the plate are then washed with PBS-A and then blocked with 10% calf serum, 90% CMF-PBS.

<Au: PBS-A OK instead of PBSA?

Yes PBS-A

<Au: Pls. provide manufacturer.

This was already included in the Materials section (see 2.3.6) Biomedia

Job: Tuan 3 (576-X)
Chapter: 40/Underhill
Pub Date: 11/99

Operator: KB
Date: 7/27/99
Revision: 1st gal/rough paging

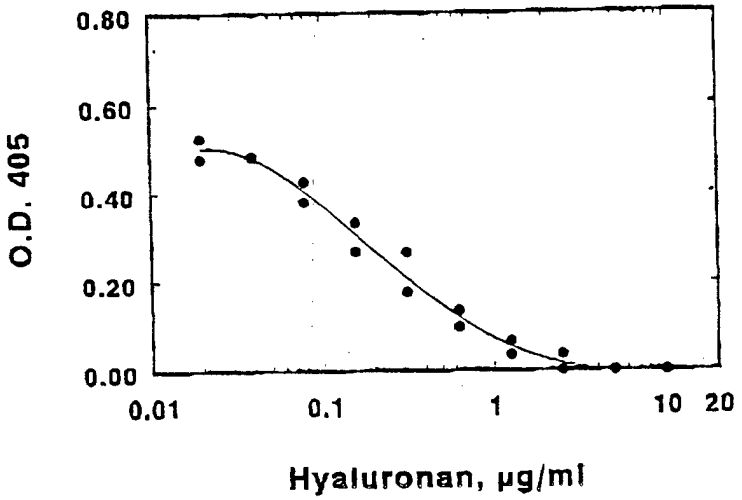

Fig. 1. Example of a standard curve for hyaluronan using the b-PG enzyme-linked assay. Varying amounts of standard hyaluronan were mixed with a set amount of b-PG and the mixtures were added to wells of a microtiter plate that had been precoated with HA-BSA. The amount of b-PG bound to the plate was then determined by the addition of peroxidase-labeled streptavidin, followed by a substrate for peroxidase.

2. In the next step, hyaluronan is released from the samples by digesting them overnight with trypsin or pronase (0.5 mg/mL, 37°C), which is then inactivated by heating to 100°C for 20 min. These samples, as well as a standard containing a known amount of hyaluronan, are serially diluted with PBS-A (100 µL per dilution).
3. An equal volume of 1 or 4 µg/mL b-PG in 10% calf serum, 90% PBS-A is added to each dilution and mixed for 1 h. Duplicate 50 µL aliquots of each dilution are then added to the wells of the 96-well plates that had been precoated with HA-BSA as described earlier. After shaking for 1 h, the plates are thoroughly washed with water and then incubated for 20 min with 100 µL/well of peroxidase labeled streptavidin diluted 1–500 in 10% calf serum, 90% PBS-A.
4. The plates are again washed with water and then to each well is added 100 µL of a peroxidase substrate consisting of 0.03% H_2O_2, 0.5 mg/mL 2,2' azinobis (3-ethylbenzthiazoline sulfonic acid) in 0.1 *M* Na citrate pH 4.2. After 30 min, the reaction is terminated by the addition of 25 µL/well of 2 m*M* NaN_3. The OD_{405} is determined using an ELISA reader.
5. When the OD_{405} of the standard is then plotted on semi-log paper, the curve is linear over the range from 50 ng/mL to 1 µg/mL of hyaluronan (*see* **Fig. 1**). Reading from test samples should be restricted to this central linear region. Control experiments showed that 10 µg/mL of chondroitin sulfate and heparin had little or no effect on the binding of b-PG to the plate.

4. Notes

1. The use of a Buchner funnel greatly facilitates the processing of the Sepharose. To transfer the gel from the funnel to a beaker, first allows the buffer to flow into the gel, release the vacuum, then rim the wall of the funnel with a spatula to separate the gel from the edge. Reapply the vacuum until the gel shrinks on top of the filter paper. The funnel is inverted and gel can be held as the filter paper is removed.

Job: Tuan 3 (576-X)
Chapter: 40/Underhill
Pub Date: 11/99

Operator: KB
Date: 7/27/99
Revision: 1st gal/rough paging

2. In some cases, we omit this lyophilization step, which saves a considerable amount of time. In this case, the appropriate amount of solid Hepes and Na acetate is added directly to the dialyzed extract.
3. To collect the b-PG in a minimal amount of buffer, it is important to keep a sharp interface with the guanidine buffer eluting the gel. To accomplish this, allow the 3 *M* NaCl to run into the top of the gel and then apply the 4 *M* guanidine to the top of the gel by inverting a 10-mL pipet so that the large opening is on the bottom.
4. Freeze thawing of the b-PG preparation in the absence of glycerol leads to a significant loss of binding activity.
5. Several factors influence the staining of hyaluronan with b-PG. First, the b-PG will only stain hyaluronan that is available to it. For this reason, the hyaluronan in cartilage does not stain because it is already complexed with proteins. Second, the hyaluronan may be lost from the section. When the synovial cavity is stained histochemically, no staining is observed because the hyaluronan is lost from the section.

Acknowledgment

This work was supported by the USAMRMC under grant number DAMD17-94-J-4173.

References

1. Green, S. J., Tarone, G., and Underhill, C. B. (1988) Distribution of hyaluronate and hyaluronate receptors in the adult lung. *J. Cell Sci.* **89**, 145–156.
2. Underhill, C. B., Nguyen, H. A., Shizari, M., and Culty, M. (1993) CD44 positive macrophages take up hyaluronan during lung development. *Dev. Biol.* **155**, 324–336.
3. Knudson, C. B. and Toole, B. P. (1985) Fluorescent morphological probe for hyaluronate. *J. Cell Biol.* **100**, 1753–1758.
4. Ripellino, J. A., Klinger, M. M., Margolis, R. U., and Morgolis, R. K. (1985) The hyaluronic acid binding region as a specific probe for the localization of hyaluronic acid in tissue sections. *J. Histochem. Cytochem.* **33**, 1060–1066.
5. Tengblad, A. (1979) Affinity chromatography on immobilized hyaluronate and its application to the isolation of hyaluronate binding proteins from cartilage. *Biochim. Biophys. Acta* **578**, 281–289.
6. Cambiaso, C. L., Goffinet, A., Vaerman, J.-P., and Heremans. J. F. (1975) Glutaraldehyde-activated aminohexyl-derivative of Sepharose as a new versatile immunoadsorbent. *Immunochemistry* **12**, 273–278.
7. Lin, W., Shuster, S., Maibach, H. I., and Stern, R. (1997) Patterns of hyaluronan staining are modified by fixation techniques. *J. Histochem. Cytochem.* **45**, 1157–1163.
8. Kusakabe, M., Sakakura, T., Nishizuka, Y., Sano, M., and Matsukage, A. (1984) A polyester wax embedding and sectioning technique for immunohistochemistry. *Stain Technol.* **59**, 127–132.
9. Graham, R. C., Lundholm, U., and Karnovsky, M. J. (1965) Cytochemical demonstration of peroxidase activity with 3-amino-9-ethyl carbazole. *J. Histochem. Cytochem.* **13**, 150–158.